MODEL STUDIES FOR FAST REACTIONS FOR PET IMAGING APPLICATIONS

By

James Matthew Norden Wolfe

A Master's thesis

submitted in fulfilment of the requirements

for the award of

Master of Science

University of East Anglia

12th September 2011

ABSTRACT

Positron emission tomography (PET) imaging is a quickly developing area of research that allows non-invasive visualisation of molecular processes *in vivo.*[1] PET imaging offers a three dimensional image with picomolar sensitivity of the processes in the body. This technique requires the development of specific molecules with high affinity for the process to be examined with the incorporation of a radiolabel, usually a short-lived positron emitting radionuclide such as ^{11}C, ^{13}N, ^{15}O, ^{18}F. The half-life of the radionuclide must allow chemical incorporation and purification of the target molecule.

In this investigation, two such probes are being studied to establish rapid reactions for the key steps that introduce the radioisotopes. This requires model studies and/or revised synthetic routes to target molecules that will interact with the muscarinic acetylcholine receptor.[2,3] Imaging based on such receptors has applications with Alzheimer's disease (AD) which is the most common neurodegenerative disease, involving the gradual and progressive memory loss and dementia.

CONTENTS

PREFACE

The research described within this thesis is, to the best of my knowledge, original and my own work, except where due reference has been made.

James Matthew Norden Wolfe
University of East Anglia, September 2011

ACKNOWLEDGEMENTS

I would like to thank my supervisors Dr. G. R. Stephenson and Prof. R. Bureau for their guidance, advice, encouragement and support throughout this research project. I am indebted to the past and present members of the "Stephenson Group" in particular Dr. Ken Hamilton for his helpful discussions and support.

I extend my thanks to Dr. Cécile Perrio, Laboratoire de Développements Méthodologiques en TEP, Cyceron, who has offered invaluable advice into this new area of research for our group.

I would also like to thank the technical staff at the department, whose names there are too many to mention for their assistance throughout this research period.

I am grateful to my friends in the organic section who have shared the burden with continuous support and humour. They include Ian Strutt, Oliver McGaw, Ketan Panchal, Dave Day, Chris Bartlett, Chris Pearce, Tony Abou-Fayad, James Tonkin, Paulina Glowacka, Becky Turner, Doyle Cassar, Adam Barter and Julien Doulcet. I would like to make a special mention to Dr. Yohan Chan who has offered a great deal of support to me and the research project.

I would like to thank my parents Simon and Stephanie, and my partner Katie who have provided endless support and belief.

Finally, my thanks to Interreg for the funding that allowed this research to be carried out.

CHAPTER ONE

MODEL STUDIES FOR FAST REACTIONS FOR PET IMAGING APPLICATIONS

1.0 POSITRON EMISSION TOMOGRAPHY

Molecular imaging is a rapidly developing area of research allowing the visualisation and characterisation of biological processes *in vivo* without the need for invasive surgery. Positron emission tomography (PET) is one such quantitative technique offering picomolar sensitivity using radiolabelled probes to target the desired biological process.

PET imaging is used both in research and clinical medicine, in particular in the fields of oncology, neurology, cardiology, psychiatry and pharmacology. PET imaging has important applications in the field of drug design with the characterisation of target molecules *in vivo*, visualising bioavailability, metabolism and metabolite distribution. PET imaging is an attractive technique as only small quantities of tracer are required to generate images; this has significant benefits to patients as toxic effects of drugs are reduced at low dose.

The idea of emission tomography was first proposed by David Kuhl and Roy Edwards in the 1950s with their work leading to the design and construction of tomographic instruments. This work was developed further by many individuals; the contributions of Gordon Brownell, William Sweet and Charles Burnham led to the first demonstration of annihilation imaging for use in medicine.

Positron emission is a type of beta decay, or β^+ decay, whereby a proton is converted into a neutron, positron and a neutrino, as summarised in Scheme 1.0.[4]

$$^{11}_{6}C \longrightarrow {}^{11}_{5}B + e^+ + \nu_e + 0.96\ \text{MeV}$$

Scheme 1.0 Equation describing β^+ decay of ^{11}C to ^{11}B

The positron emitted through this process slows in speed before undergoing an annihilation reaction between the positron and electron in the shell of a neighbouring atom. Typically this is in the order of one millimetre in distance from the point of beta decay. Upon annihilation two gamma rays with energy 511 keV are produced travelling in diametrically opposing directions. These gamma rays are detected by a coincidence counting detection system. After a filtering process, this information is used to re-construct a cross-sectional image as depicted in Figure 1.0.

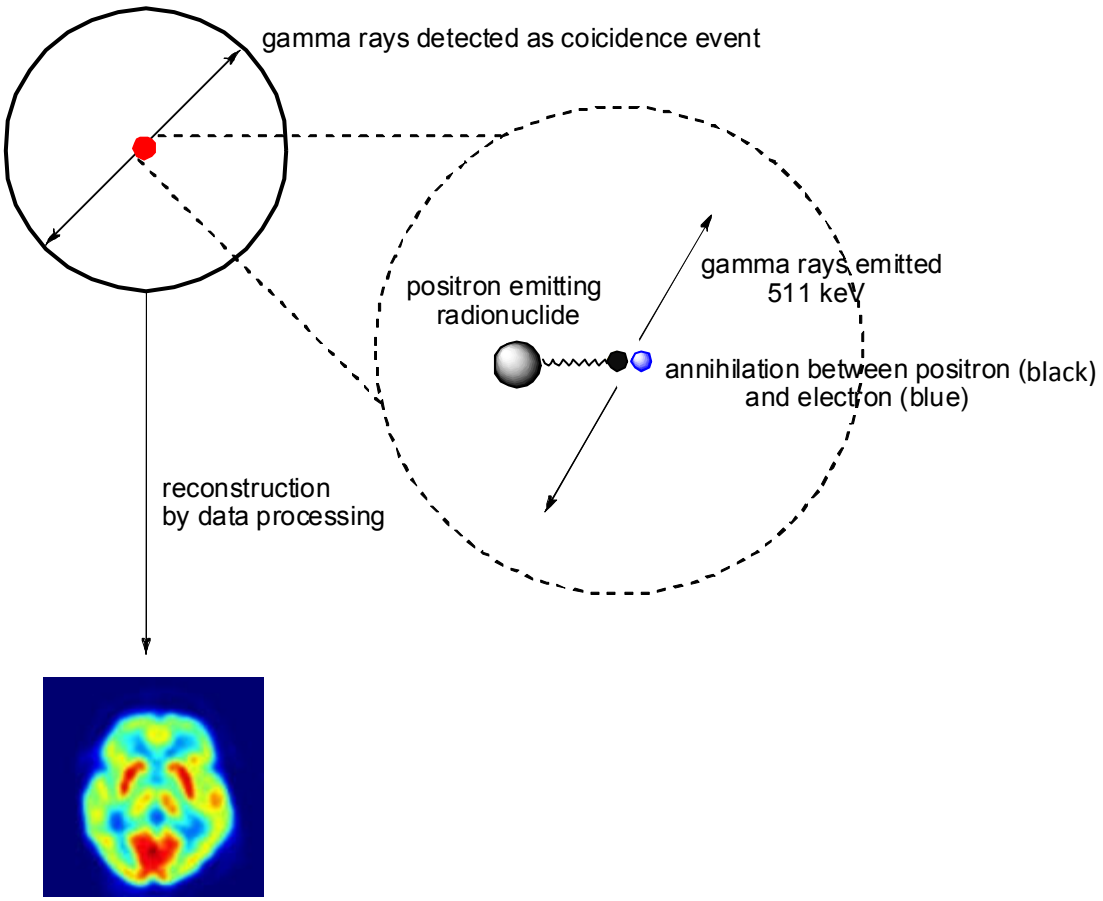

Figure 1.0 Overview of PET scanning process[5]

The majority of radionuclides are artificially produced in a cyclotron reactor. More than 300 nuclides are known of which 270 are stable and the remainder are radioactive. In PET imaging, only positron-emitting radionuclides are required, and relatively few positron-emitting radionuclides have been successfully utilised in clinical applications. These radionuclides include ^{11}C, ^{13}N, ^{18}F, ^{15}O. These radionuclides are produced in a medical cyclotron usually on site at the point of administration due to their short half-lives.

Medical cyclotrons are compact cyclotrons that are primarily used to produce short-lived radionuclides, by nuclear reactions using low-energy particles. Commonly in medical cyclotrons hydride ions, H^-, are preferred as the cyclotron housing does not become radioactive as is the case with positive ion cyclotrons.

Some of the most common PET nuclides and their characteristics are given in Table 1.0. The radionuclides are short lived; this puts limitations on the synthesis time for PET radiopharmaceuticals. However, the attractive advantage of using such radionuclides is that the ligands (radiolabel) can be incorporated into biological

receptors and therefore often depict a true representation of biological processes *in vivo*.

Nuclide	Physical half-life ($t_{1/2}$)	Mode of decay (%)	γ-ray energy (keV)	Abundance (%)
^{11}C	20.4 min	β^+ (100)	511	200
^{13}N	10 min	β^+ (100)	511	200
^{15}O	2 min	β^+ (100)	511	200
^{18}F	110 min	β^+ (97)	511	194

Table 1.0. Characteristics of common positron emitters

Perhaps the most well known examples are ^{18}F-fluorodeoxyglucose (FDG) (Scheme 1.01) which is used as an analog of glucose for cellular metabolism and $H_2{}^{15}O$ for cerebral perfusion.

The first synthesis of ^{18}F-FDG was carried out by Wolf *et al.* in 1976 via electrophilic fluorination. The synthesis subsequently carried out by Fowler *et al.* is depicted in Scheme 1.01.[6,7]

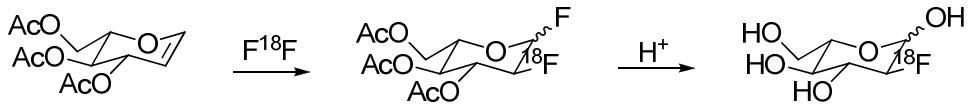

Scheme 1.01 Synthesis of ^{18}F-FDG

The electrophilic fluorination carried out by Fowler *et al*. involved the use of 4, 6-tri-*O*-acetyl-D-glucal as the precursor. The glucal was treated with F_2 (with mono substituted fluorine-18) to yield a 3:1 mixture of the desired difluoro-glucose and the undesired difluoro-mannose. The difluoro-glucose was separated and hydrolysed to yield 2-fluoro-2-deoxyglucose (FDG) in 8% yield in two hours.[7,8] Despite a long synthetic process and low yield they went on to map glucose metabolism in the brain, constituting the first human trial of ^{18}F-FDG.[6,7]

Fluorine-18 is widely preferred since it has a relatively long half-life that allows production and distribution to remote locations. In all examples of radiopharmaceuticals, a suitable synthetic method is designed to provide a stable

product with good labelling yield, high specific activity, high purity and perhaps most importantly high *in vivo* tissue selectivity.

Fluorine-18 is produced by irradiation of ^{18}O-water with 10 to 18 MeV protons in a cyclotron and recovered as ^{18}F-sodium fluoride by passing the irradiated water target mixture through a carbonate type anion exchange resin column. The water passes through and the $^{18}F^-$ is trapped on the column. This can be subsequently recovered by washing with potassium carbonate solution to form a solution of $K^{18}F$.

Oxygen-15 can be prepared as ^{15}O-water and *n*-^{15}O-butanol. The former is prepared in the cyclotron by the $^{15}N(p,n)^{15}O$ (or $^{14}N(d,n)^{15}O$) reaction. The irradiated gas is transferred to a ^{15}O-water generator in which ^{15}O is combined with hydrogen over a palladium/charcoal catalyst at 170°C.[9,10,11] The resulting $H_2{}^{15}O$ vapour is trapped in saline and passed through a membrane filter. The sample is often injected online straight into the patient given the short timeframe in which it is necessary to work.

The latter, *n*-^{15}O-butanol, is prepared by the reaction of ^{15}O (preparation described above), with tri-n-butylborane loaded on an alumina Sep-Pak cartridge. ^{15}O-butanol is eluted from the cartridge with ethanol/water.[11,12]

Nitrogen-13 has been isolated as ^{13}N-ammonia, produced by the reduction of ^{13}N-labelled nitrates and nitrites from the proton irradiation of water in a cyclotron. The reduction is carried out in in alkaline conditions. ^{13}N-ammonia can then be distilled and trapped in saline solution under acidic conditions.[11,13] The resulting solution is then purified through anion exchange resins and passed over a membrane filter. Careful control of the pH is required to remain between 4.5 and 7.5.

Carbon-11 can be prepared as ^{11}C-CO_2, and thus used to prepare a variety of different compounds that include: ^{11}C-sodium acetate, ^{11}C-flumazenil, ^{11}C-*L*-methionine, ^{11}C-raclopride and ^{11}C-methylspiperone (MSP) (Figure 1.01). One of the common radiolabel precursors is the use of ^{11}C-iodomethane for *N*-methylation. ^{11}C-MeI is prepared from the reduction reaction of $^{11}CO_2$.

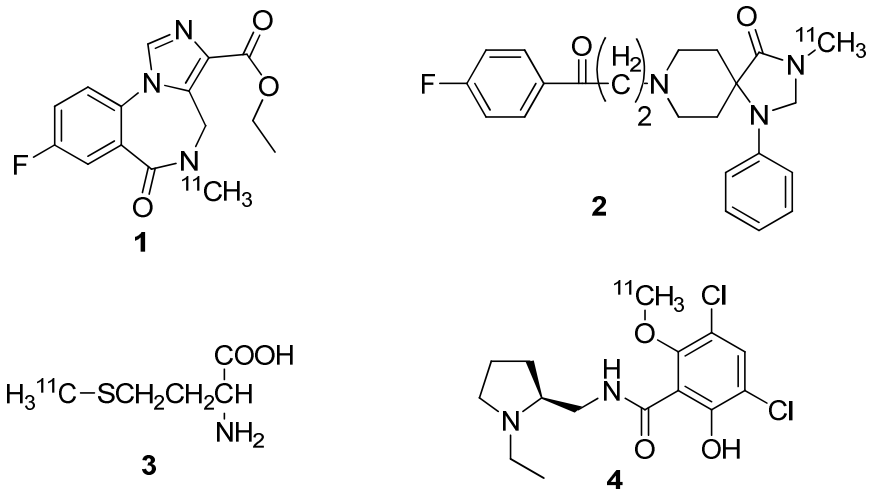

Figure 1.01 Molecular structures of ^{11}C-flumazenil (1), ^{11}C-methylspsperone (MSP) (2), ^{11}C-*L*-methionine (3), ^{11}C-raclopride (4)

The first step in developing new probes for positron emission tomography is the identification of the target, which generally consists of an enzyme, a transporter or a receptor.[1,14] Once the target has been identified, ligands for the target need to be selected, either by rational design based on structural biology[1,15] or by high throughput screening of libraries of compounds, or by a combination of both. In the latter case, libraries are generally selected based on rational design to speed up the process by limiting the number of compounds to be screened.[1,16]

Our approach to choosing targets for this project is based on the idea of "mining" published but non-commercialised pharmaceutical agents. Such a selection process could identify target molecules suitable for use as PET contrast agents from the pool of pharmaceutical compounds that have failed clinical trials for therapeutic treatment of conditions because of problems with toxicity, efficacy, etc.

While such compounds may not be suitable for treatment of chronic/acute conditions due to toxic or adverse events over an extended period of time, such a target may exhibit the required specificity and affinity for a particular enzyme or receptor which would make it suitable as a PET contrast agent given it is delivered as a single low dose. Similarly, while a particular compound may not exhibit the required efficacy to progress onto further clinical trials and become an effective treatment for a given condition, it is not to say these compounds do not have again the required specificity and affinity for a given biological process that would make it suitable as a PET contrast agent.

On this basis, the compounds discussed below have been chosen from classes of compounds that have not been developed into therapeutic treatments but have been shown to possess good affinity and specificity for their respective receptors. Clearly this type of methodology of screening the vast numbers of drugs that have failed clinical trials would almost certainly generate huge libraries of compounds, and to consider each target in turn is beyond the scope of this project. Consequently, it was decided to aim our efforts at a particular disease area to refine the selection process. Thus, our efforts were focused on Alzheimer's disease (AD) for reasons of potential collaboration with other groups with a similar interest through the Interreg program and Innovative Synthesis, Culture and Entrepreneurship (IS:CE).

1.1 ALZHEIMER'S DISEASE

Increasing life expectancy of the population makes Alzheimer's disease (AD) a growing public health problem, so there is great need to find ways to prevent and delay the disease.[17] AD is a progressive, neurodegenerative disease accounting for 60–70% of dementia cases in the elderly with no current modifying treatment.[16] AD disease accounts for most cases of dementia that are diagnosed after the age of 60 years. It affects 20–30 million individuals worldwide.[18,19] The prevalence of AD increases with age and life expectancy is constantly increasing in developed countries, it has been predicted that the incidence of AD will increase threefold over the next 50 years.

The progression of AD is different for each individual; however there are similarities in the symptoms experienced by sufferers with patterns in cognitive and functional impairments. Symptoms often include memory loss, confusion, irritability, language breakdown, aggression and withdrawal. The earliest symptoms are commonly mistaken for the natural progression of ageing or stress, given that memory loss is common to all ageing individuals.[20]

As the disease progresses patients require increasing levels of care, and often patients present with increasing severity of symptoms to the point of fatality. Currently no cure is available for AD so the primary concern is the management of patient symptoms that falls to a carer. This has a significant impact on such a care giver, often a spouse or relative, with respect to physical, psychological and economic burden.[21,22] AD accounts for the highest economic burden on society in developed countries.[22,23]

The cause and progression of AD is not currently understood. Most recent research has been directed into clinical markers associated with the disease and risk factors associated with the onset of AD. It is thought the disease is associated with amyloid plaques and tangles found in the brain.[22,24] While the complete prevention of AD is unlikely with our current understanding, there are lifestyle habits that are thought to slow the onset and progression of the disease with exercise, balanced diet and mental stimulation that have been found to slow the onset of AD.[22,25]

"Finding AD risk-factor genes is essential for understanding the very early biological steps that lead to the vast majority of AD cases and for developing drugs and other prevention and treatment strategies. Finding these genes also will help scientists develop better ways to identify people at risk of AD and determine how the

genes may interact with other genes or with lifestyle or environmental factors to affect an individual's AD risk".[25]

1.2 AIMS OF THE PROJECT

In this investigation we set out to achieve the development of a route to PET contrast agents by offering a robust synthetic protocol to allow the incorporation of carbon-11 radionuclides by selective *N*-alkylation of pyridine rings and subsequent regioselective reduction to yield 1-alkyl-tetrahydropyridine moieties. Offering this protocol would allow the synthesis of a wide variety of compounds to gain new insight into the target M_1 muscarinic receptor and its effect on the progression of AD.

Once we have established a general protocol we will look to synthesise an example of an M_1 muscarinic receptor agonist, based on current publications, to demonstrate the application of the developed protocol as well as gaining experience with the challenges of synthesising PET contrast agents.

CHAPTER TWO

2.0 MUSCARANIC RECEPTOR

Muscarinic acetylcholine receptors (mAChRs) are G protein-coupled acetylcholine receptors found predominantly in the plasma membranes of neurons and other cells. They play various roles predominately mediating the metabotropic (signal transduction) action of acetylcholine. Muscarinic receptors are classified into five sub-types M_1-M_5, their location and function is given in Table 2.0.

mAChRs sub-type:	Location:	Function:
M_1	• Central nervous system (CNS)	• secretions from salivary glands • memory
M_2	• CNS • heart	• slow heart rate • reduce contraction force of atrium • reduce conduction speed of AV node
M_3	• CNS • eye • digestive system • muscular system	• smooth muscle contraction • vasodilation • secretions from endocrine/exocrine glands • induce emesis
M_4	• CNS	• enhance locomotion
M_5	• CNS	• not fully understood

Table 2.0 Location and function of mAChRs sub-types in human body[26,27]

Muscarinic acetylcholine receptor subtypes have been the subjects of research for at least a quarter of a century. Nonetheless, there are few selective muscarinic receptor ligands presently used as therapeutics.[28] There has been extensive research into the role of M_1 mAChR agonists and their effect on cognitive dysfunctional conditions such as AD, but as yet no successful drug candidate has been developed from such research suggesting a lack of understanding of the role played by M_1 mAChRs in dementia.

Highly selective mAChRs subtype antagonists have been developed - the best of which were extracted from snake venom.[29] However, with the exception of pirenzepine (Figure 2.0), few have been further developed into novel therapeutic treatment for cognitive dysfunction.[30,31]

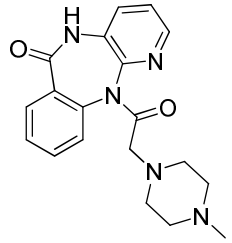

Figure 2.0 Structure of pirenzepine, mAChRs M_1 antagonist

By contrast, M_1 selective mAChRs agonists have been developed with initial success for the treatment of AD, and also other conditions associated with cognitive dysfunction. The M_1 mAChRs are widely found in the CNS (Table 2.0), located predominately in the cortex and hippocampus, and are known to be associated with learning and memory.[32] Both of these areas have been established as areas of the brain that develop amyloid plaques during the progression of AD. As such M_1 mAChRs have been identified as a potential therapeutic target since AD is known to progress through a decreased activity in cholinergic activity in the brain thus reducing functional signalling capacity in the brain. It has been shown that this decrease in cholinergic activity is not due to depletion in mAChRs G-protein coupled receptors but rather a decrease in the number of receptors in an agonist stimulated state.[33,34]

Many pharmaceutical companies have pursued the development of specific M_1 mAChRs agonists for the treatment of cognitive dysfunction, including arecoline, cevimeline, tazomeline, alvameline, talsaclidine, xanomeline, milameline and sabcomeline. While many of these compounds progressed to pre-clinical trials showing good efficacy towards cognitive dysfunction, many were withdrawn either due to poor side effect profiles or unacceptable safety margins.

Such side effects in general arise from not only the stimulation of M_1 subtypes but also M_2 and M_3 subtypes. Candidates experienced associated cholinergic side effects including salivation, lacrimation and gastro-intestinal disturbances.[35] Low doses administered to candidates in an attempt to limit possible side effects were not found to possess sufficiently satisfactory efficacy to proceed into clinical trials. This

demonstrates a further lack of understanding in the development of selective M_1 mAChRs agonists.

Most of the compounds given above are derived from arecoline (Figure 2.01), an alkaloid natural product found in the areca nut of the areca palm. Arecoline itself is a partial agonist of M_1, M_2 and M_3 mAChRs subtypes and as such has been shown to improve memory in AD patients. However, is not recommended due to its possible carcinogenic effects.[36,37]

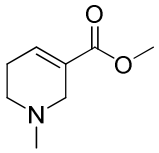

Figure 2.01 Structure of arecoline

Arecoline was first synthesised in 1951 by J. J. Panouse[38] from nicotinic acid, and then subsequently optimised by N. Kinoshita in 1962[39] and I. A. Kozello in 1976.[40] The reaction scheme for Kozello's synthetic strategy is depicted in Scheme 2.0.

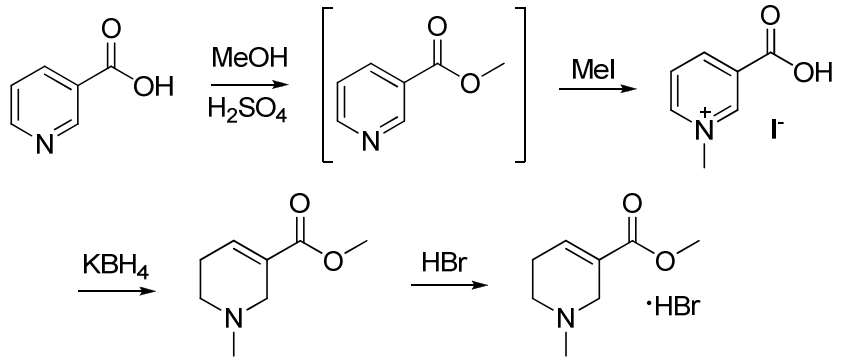

Scheme 2.0 Synthesis of arecoline hydrogen bromide

Importantly, all three authors used potassium borohydride to selectively reduce the pyridine ring to yield the desired allylic ester. In the first instance, Panouse and Kinoshita carried out this reduction in methanol with 32-36% yield.[40] Kozello improved on their original strategy by carrying out the reduction in water under a layer of benzene with an improved yield of 42%.[40]

Since the work by Kozello *et al.* on the synthesis of arecoline numerous investigations have been carried out to evolve from the natural product to an M_1 selective agonist. It is the work that is summarised below which gives an overview of the origin of the target molecule to date.

Some of the first modifications to arecoline were carried out by Sauerberg *et al.* in 1992, with investigations into the synthesis and structure-activity relationship (SAR) of 3-(1,2,5-thiadiazoyl)-1,2,5,6-tetrahydro-1-methylpyridines.[41] A wide variety of molecules were synthesised and evaluated with SAR primary measure being IC_{50} (nM) of receptor binding in rat brain membrane. The most promising molecules and their syntheses are summarised in Scheme 2.01. As well as the molecules shown in Figure 2.03, furan and oxazole rings were also investigated. However it was found this resulted in a decrease in affinity for the M_1 receptor.

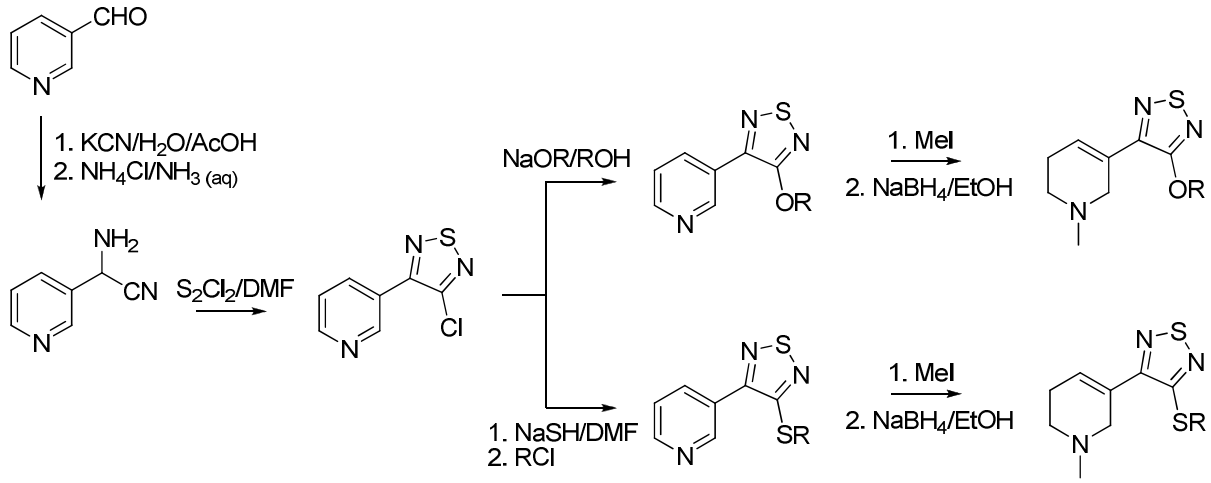

Scheme 2.01 Summary of synthetic strategy of alkoxy/alkylthio thiadazole derivatives of arecoline[41]

A variety of alkyl substituents were investigated for R, and it was found that unbranched, short alkyl substituents gave the best selectivity for M_1 receptor. Both types of molecule demonstrated promising selectivity with minor peripheral side effects in rat and guinea pig models, making them potential candidates for the treatment of AD.

At approximately the same time, work was being carried out by Ward *et al.* on behalf of Lilly Pharmaceuticals into developing arecoline in a very similar manner to Sauerberg.[42] The three molecule models of interest are given in Figure 2.01, with their general synthetic strategy in Scheme 2.02.

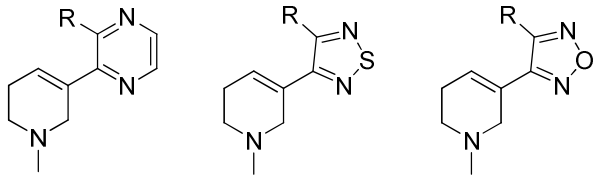

Figure 2.01 Synthetic models for M_1 receptor agonist[42]

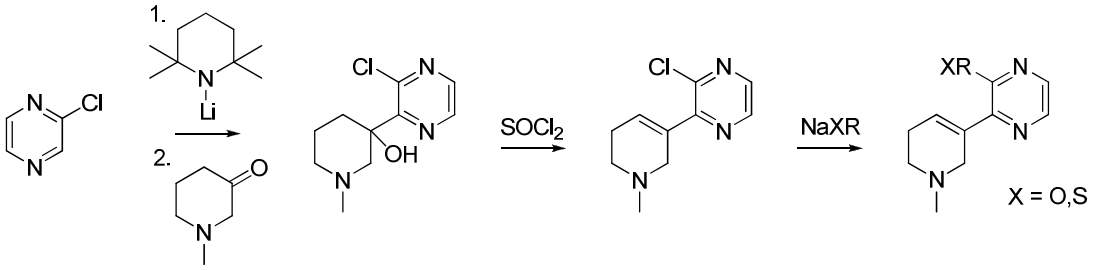

Scheme 2.02 General synthetic strategy for synthesis of l-Methyl-l,2,5,6-tetrahydropyridyl-1,2,5-thiadiazolee, -pyrazines, and -l,2,5-oxadiazoles[42]

By comparison of the work carried out by Sauerberg and Ward we see distinct similarities in the backbone of the molecule. Both series of molecules include 1-methyl-1,2,5,6-tetrahydro pyridine rings, as does arecoline. This suggests an important motif to the selectivity of the molecules for M_1 receptor. In addition to this, both papers focused on the use of heterocyclic ring systems in place of the ester of arecoline.

Their respective approaches to the synthesis of such molecules are somewhat different. Sauerberg opted for a synthetic strategy more in line with the original synthesis of arecoline whereby they started from a pyridine derived molecule and installed the desired heterocyclic ring system plus any required functionality followed by *N*-methylation and regioselective reduction of the pyridine ring. By contrast Ward opted for a synthesis that involves a functionalisation of the alcohol at the piperidine ring to yield the desired alkene before introducing the desired functionality on the heterocyclic ring.

The binding affinities were assessed by the displacement of radiolabelled compounds already occupying the muscarinic receptor. This approach is perhaps somewhat problematic given that it gives no insight into metabolism of the target molecule, bioavailability or additional binding interactions beyond the target receptor. However this does demonstrate the use of such radiolabelled compounds with respect to drug design that is convenient to measure *in vivo* affinity. To address this

problem we carried out a molecular modelling investigation into the muscarinic receptor discussed further in chapter three.

More recently, the development of such molecules has led to derivatisation with morpholine. Morpholine is found in many naturally occurring products and drugs but is often restricted in its use as it is often accessed via amino alcohols or amino epoxides.[43] Introduction of chirality into morpholine derived compounds is often achieved by starting from enantiopure amino alcohols, frequently from the naturally occurring chiral pool. As such this puts a limitation on the number of accessible morpholine compounds.

As a result, morpholine is more frequently used as a base or *N*-alkylating agent. *C*-functionalised morpholine is much less explored but offers great potential given its frequent occurrence in nature.[43]

With this in mind more recent publications of selective M_1 agonists incorporating *C*-functionalised morpholine have been put forward. The first generation of such a compound was synthesised by Kumar *et al.* in 2007.[44] The synthesis of the arecoline derived compound was achieved in nine steps in good yield (Scheme 2.03)

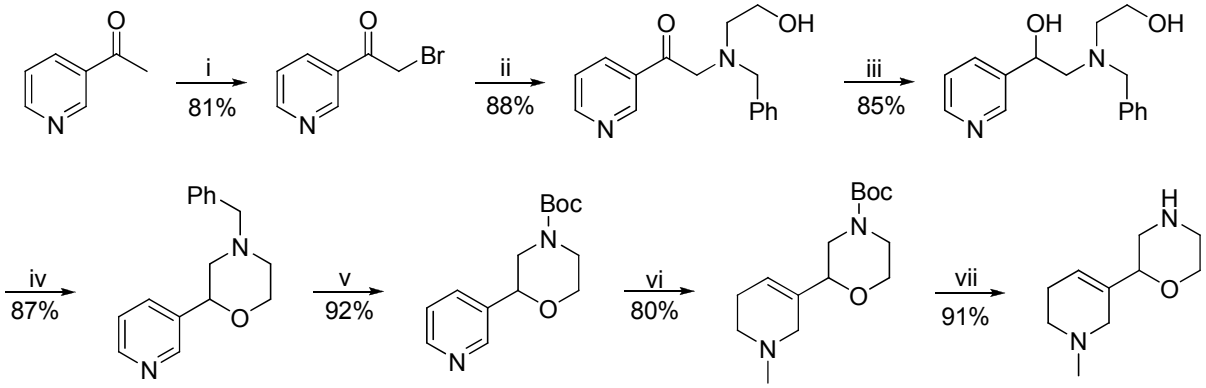

Reagents: (i) HBr, acetic acid (ii) *N*-benzylaminoethanol, K_2CO_2, DMF (iii) $NaBH_4$, MeOH (iv) H_2SO_4, reflux (v) a) 10% Pd-C, ammonium formate, MeOH, reflux b) $(Boc)_2O$, THF, K_2CO_2 (vi) a) MeI, acetone b) $NaBH_4$, MeOH (vii) HCl, MeOH

Scheme 2.03 Synthesis 2-(1-methyl-1,2,5,6-tetrahydropyridin-3-yl)morpholine[44]

This general synthesis gives access to *C*-functionalised morpholine substituted arecoline derived compounds with an overall yield of 36% from the starting acetyl pyridine to the final product. This compound was evaluated as a potent, selective M_1 agonist.[44] This synthetic strategy offers possible further derivitisation at the secondary amine of the morpholine ring that were subsequently

synthesised and evaluated as described below. It is worth noting the similarities to the original synthesis of arecoline with the final steps including *N*-methylation and subsequent reduction with sodium borohydride. While the use of potassium borohydride was described in the original synthesis, sodium borohydride was shown to give an improved yield in this case.

To further derivatise the secondary amine this work was continued with a publication by the same group in 2008.[45] The work focused on the synthesis of sulfonyl derivatives with a variety of electron donating and withdrawing properties. The general approach for the synthesis follows that described in Figure 2.06 with subsequent derivatisation described in Scheme 2.04.

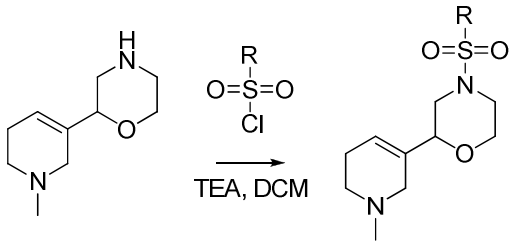

Scheme 2.04 Synthetic approach to sulfonyl derivatives of morpholino arecoline[45]

The 4-substituted aromatic sulfonyl substituents (Figure 2.02) resulted in a 50 to 80 fold increase in M_1 receptor binding when compared to arecoline.

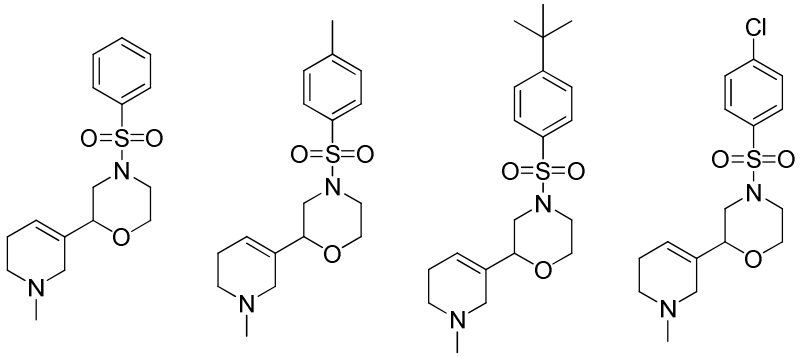

Figure 2.02 M_1 selective 4-substituted 2-(1-methyl-1,2,5,6-tetrahydropyridin-3-yl)-4-(phenylsulfonyl)morpholine derivatives

Interestingly, the effects of electron withdrawing substituents were investigated by Kumar. It was found that nitro-substituents at *ortho* and *para* positions notably decreased the affinity of the compound to M_1 receptor as compared to those examples given in Figure 2.02. This decrease in affinity was observed to a

lesser extent in the *meta* position, due to the less withdrawing effect at the *meta* position.

One of the most important findings was that the toxicity of all the compounds synthesised and evaluated by Kumar e*t al.* was low with no visible side effects observed in rat brain models.[45] By contrast to some of the earlier work discussed previously, this represents a promising development towards a highly selective M_1 receptor agonist.

In a similar vein Malviya *et al.* carried out further investigations into the synthesis and evaluation of *N*-arylthiourea morpholine arecoline derivatives.[46] Again the synthesis followed that given in Scheme 2.03 followed by derivatisation via Scheme 2.05.

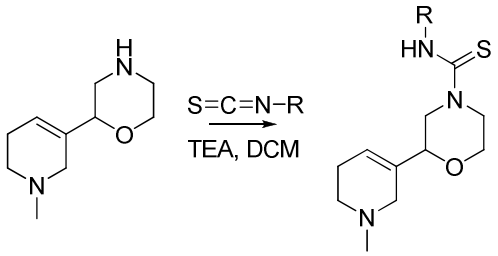

Scheme 2.05 Synthetic approach to arylthiourea derivatives of morpholino arecoline[46]

Again a variety of compounds were synthesised and evaluated in the same fashion as the work previously discussed showing a several fold increase in affinity as compared to arecoline.[46] The best examples from this investigation are given in Figure 2.03. No direct comparison is given for the respective affinities between the sulfonyl and arylthiourea derivatives; however from the detailed IC_{50} values the sulfonyl derivatives show marginally improved affinity.

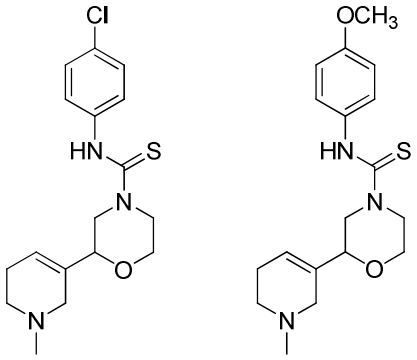

Figure 2.03 M_1 selective 4-substituted 2-(1-methyl-1,2,5,6-tetrahydropyridin-3-yl)-N-phenylmorpholine-4-carbothioamide[46]

In more recent publications Sadashiva *et al.* proposed the synthesis and biological evaluation of *N*-alkyl/aryl thiazolidinone arecoline derivatives. This constitutes a move back to much earlier examples of arecoline derived compounds similar to that of Sauerberg previously described.[41]

A novel synthetic strategy to access *N*-alkyl/aryl thiazolidinone arecoline derivatives was proposed from the same starting material as Sauerberg. 3-Pyridine carboxaldehyde was reacted with a variety of different amines in the presence of the catalyst γ-ferrite (Scheme 2.06).[47]

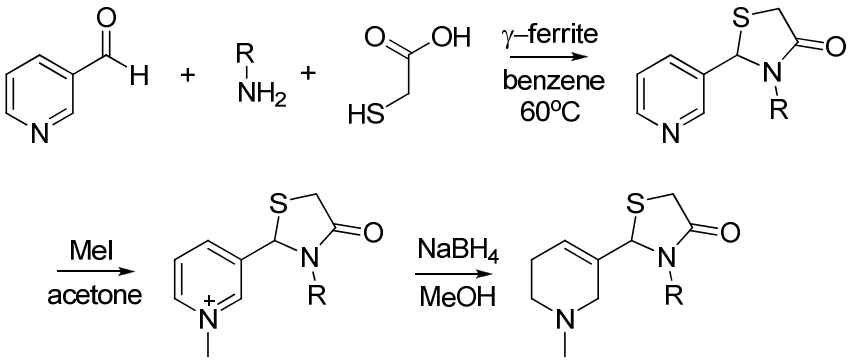

Scheme 2.06 Synthetic strategy to *N*-substituted thiazolidinone derivatives

The compounds synthesised with the reported highest affinity are given in Figure 2.04. All the compounds synthesised were subjected to the same biological evaluation that was carried out by Kumar *et al.* and Malviya *et al*.[47]

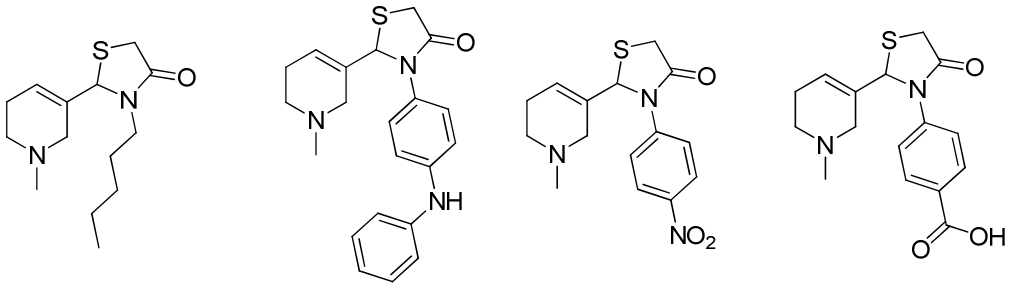

Figure 2.04 M_1 selective *N*-substituted 2-(1-methyl-1,2,5,6-tetrahydropyridin-3-yl)thiazolidin-4-one derivatives

It was noteworthy that as with the morpholine substituted compounds no cholinergic toxicity was observed at comparable doses.[47] However, the measured affinity for M_1 receptor was poor by comparison to the morpholine arecoline derivatives already discussed. More in depth *in vitro*/*vivo* studies need to be carried

out to strengthen the suitability of this class of molecules as a selective therapeutic M_1 receptor agonist.

The most recent work carried out by Malviya *et al.* in 2009 built on their previous publications and looked to synthesise and evaluate novel *N*-aryl carboxamide substituted morpholine arecoline derived compounds.[2] The results suggest that *para* substituted methyl aromatic amide moieties (Figure 2.05) exhibit selectivity towards M_1 receptor with anti-dementia activity.

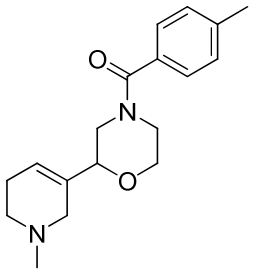

Figure 2.05 Structure of (2-(1-methyl-1,2,5,6-tetrahydropyridin-3-yl)morpholino)(p-tolyl)methanone[2]

The synthesis is again based on the strategy developed in the previous publication (Scheme 2.03) followed by reaction with the corresponding acid chloride (Scheme 2.07).

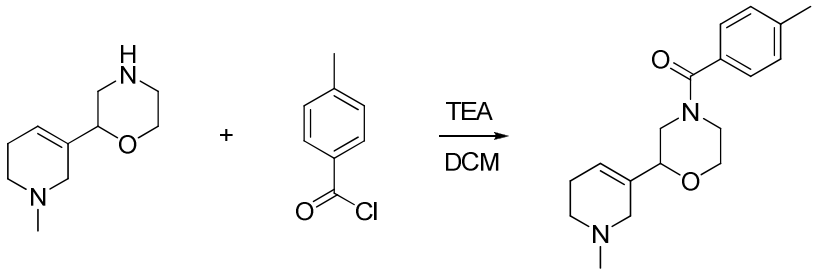

Scheme 2.07 Synthesis of (2-(1-methyl-1,2,5,6-tetrahydropyridin-3-yl)morpholino)(p-tolyl)methanone[2]

This reaction has been common to all of the syntheses by Malviya *et al.* and Kumar *et al.* of a variety of substituted morpholine arecoline derived compounds.

From studies performed *in vitro* it was noted substitution at the *para* position of the aromatic ring is important for M_1 receptor activity. The same molecule with no *para* substituent was evaluated, and it was found that the affinity and potency of the compound decreased by several-fold compared to those compounds with a *para* substituent.[2] A number of substituents were investigated (Figure 2.06) and subjected

to *in vitro* affinity studies towards M_1 receptor of male Wistar rat cortex synaptosomal membrane. The results of these studies are given in Table 2.01.[2] This was the assessment of affinity used by all publications discussed.

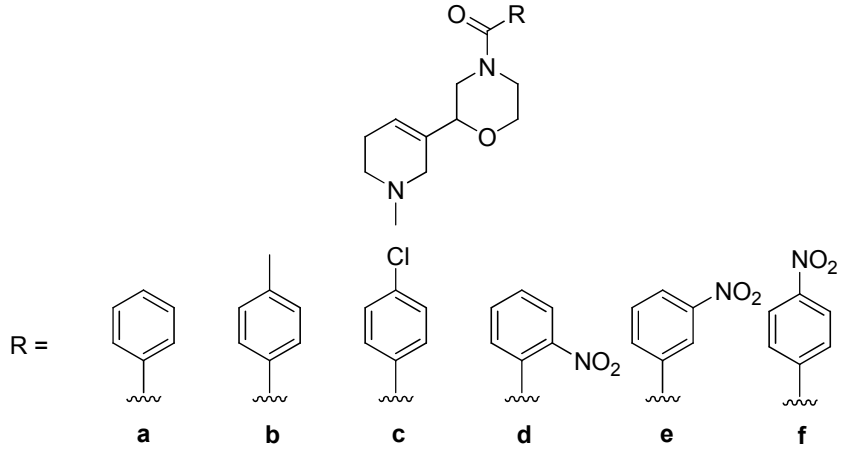

Figure 2.06 Analogues of carboxamide morpholino arecoline derived M_1 receptor agonist

Compound:	K_i (μM)	IC_{50} (μM)
a	19 ± 3.22	76 ± 5.51
b	**0.42 ± 0.06**	**1.6 ± 0.13**
c	1.3 ± 0.08	4 ± 1.50
d	126 ± 13.83	618 ± 20.35
e	48 ± 7.32	142 ± 11.14
f	65 ± 6.12	215 ± 13.50
arecoline	88 ± 11.25	460 ± 18.18

Table 2.01 In vitro affinity assay of carboxamide substituted morpholino arecoline derivatives towards M_1 receptor of male Wistar rat cortexsynaptosomal membrane.

As with previous examples none of these compounds exhibited toxic cholinergic activity with respect to visible side effects.

Compound **b** emerged as a promising derivative with anti-dementia activity. It is this derivative that forms the basis of our investigation to incorporate a radionuclide for the purposes of PET imaging. When considering a strategy towards a PET contrast agent it was important for us to consider where to incorporate the radionuclide since this will have significant bearing on the design of the synthesis. As discussed previously it is important to incorporate the radionuclide at the end of

the synthesis, termed the “hot step”, to allow chemical incorporation and purification within the half life of the radionuclide.

In this investigation we wanted to not only gain experience with the synthetic challenges of PET contrast agents, but also demonstrate a novel method for the incorporation of a radionuclide. With this in mind and combined with the appeal of offering a synthesis that could be applied to a variety of compounds within this class of M_1 receptor agonists, compound **1** was selected as the target molecule for this investigation (Figure 2.07).

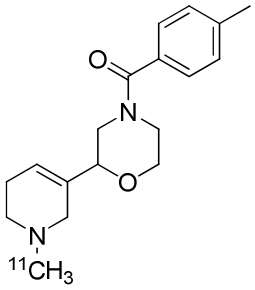

1

Figure 2.07 Proposed PET contrast agent towards M_1 receptor

Incorporation of the radionuclide at the *N*-methyl of the tetrahydropyridine ring is convenient in this case as this moiety is common to all M_1 receptor agonists discussed in this chapter. Conveniently, the original synthesis of this molecule would allow the incorporation of a radionuclide provided that the final *N*-methylation and regioselective reduction can be carried out in a short time frame of approximately 10 minutes (Scheme 2.03, step (iv)).

In the synthesis proposed by Malviya *et al.* the *N*-methylation and reduction are not detailed with respect to time taken for the reaction to complete.[2] However this chemistry has been carried out on numerous examples and proceeds in the order of 2 hours to carry out an *N*-methylation and 3 hours for the subsequent reduction. It was our challenge to condense this chemistry into 10 minutes.

2.1 TOWARDS THE SYNTHESIS OF (2-(1-METHYL-1,2,5,6-TETRAHYDROPYRIN-3-YL)MORPHOLINO)(P-TOLYL)METHANONE (1)

Before embarking on the synthesis of the target molecule (Figure 2.06) we felt it was necessary to ascertain whether the 10 minute time scale was realistic on simple models. We chose pyridine as a simple model (Scheme 2.08) to demonstrate the necessary chemistry and satisfy ourselves that it was worthwhile embarking on the synthesis of **1**.

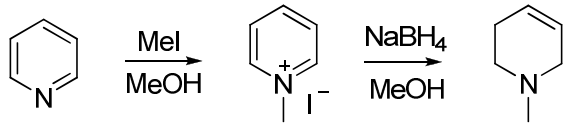

2 **3**

Scheme 2.08 Synthesis of 1-methyl-1,2,3,6-tetrahydropyridine

Initially our approach involved the synthesis of **2** and **3** individually to attempt each step in a short time scale. In the synthesis described by Malviya *et al.* the *N*-methylation was carried out in acetone.[2] We chose to carry out this reaction in methanol with a view that these steps could eventually be carried out in one pot or in flow. The reactions were carried out at varying temperatures (Table 2.02).

Time (min)	Temperature (^{o}C)	Concentration of pyridine (mol)	Concentration of MeI (mol)	Yield of **2** (% from pyridine)
120	25	0.06	0.05	62%
3	30	0.06	0.05	nil
3	35	0.06	0.05	nil
3	40	0.06	0.05	4%
3	45	0.06	0.05	7%
3	50	0.06	0.05	8%
3	55	0.06	0.05	10%
3	60	0.06	0.05	14%
3	reflux	0.06	0.05	16%

Table 2.02 Kinetic studies for *N*-methylation of pyridine

The *N*-methylation of pyridine was followed by NMR, sampled every two minutes for an eight minute period (Figure 2.08). The traces show clean conversion to the *N*-methyl pyridinium salt with no side reaction occurring.

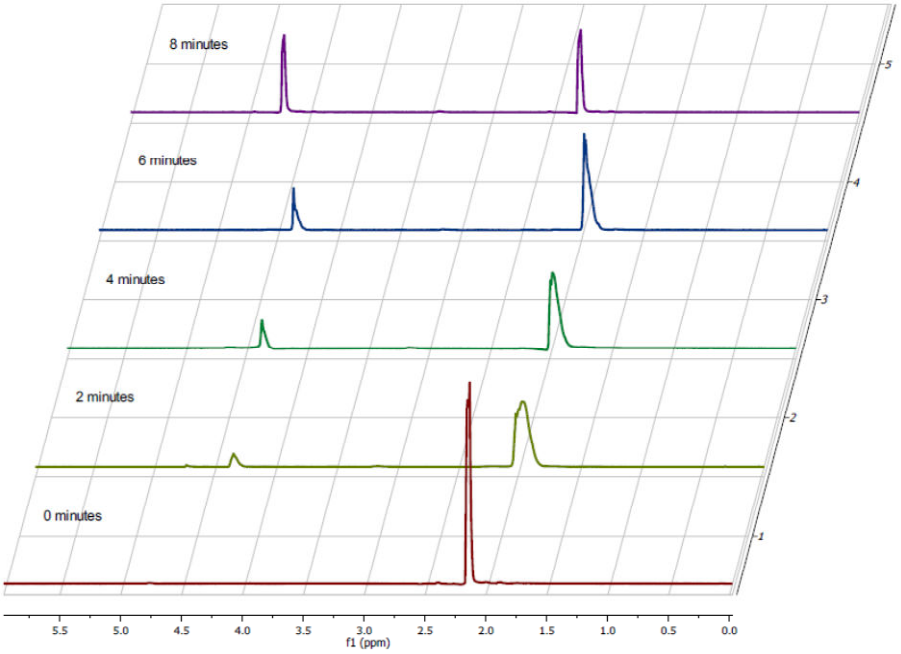

Figure 2.08 *N*-methylation of pyridine followed by NMR

While the *N*-methylation was successful with a clear increase in yield with increased temperature to a yield of 16% at reflux to a level that we felt was acceptable for our first attempt, the subsequent reduction product **3** could not be successfully isolated. This is possibly due to a low boiling point similar to that of methanol. Since we had satisfied ourselves that the *N*-methylation progresses quickly, we turned to a less volatile model to improve the yield and prove that the borohydride reduction could be carried out quickly. We decided to move to isoquinoline to model the same chemistry; this offers the distinct advantage of being able to follow the reaction easily via thin layer chromatography (TLC) (Scheme 2.09).

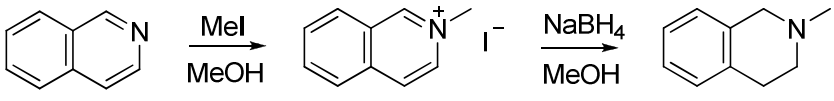

4 **5**

Scheme 2.09 Synthesis of 2-methyl-1,2,3,4-tetrahydroisoquinoline

This strategy proved successful with the *N*-methylation of isoquinoline yielding **4** in 85%. The subsequent reduction also proved successful with the reaction

proceeding initially in 20 minutes to yield **5** in 52% from **4**. Having successfully carried out the reaction with isolation of **5** we were able to repeat the step at reflux and quenching after 8 minutes yielding **5** in 27% from **4**. In light of these results we felt it was worthwhile proceeding onto a synthesis of **1**.

Our strategy was to offer a synthesis that primarily would allow the successful incorporation of a radionuclide but also an alternative synthetic route to allow access to a variety of C-functionalised morpholine derivatives if so required. Our first generation retrosynthetic analysis (RSA) of **1** is shown in Scheme 2.10.

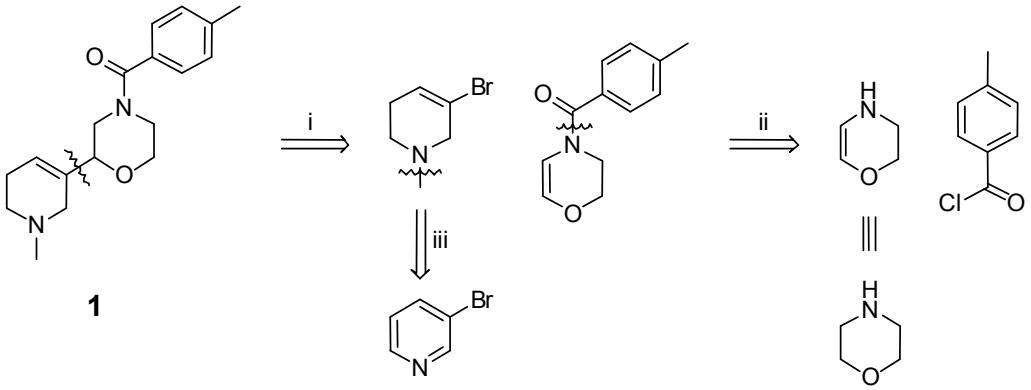

1

Scheme 2.10 First generation RSA towards **1**

In the first dissection of the C-C bond between the morpholine and tetrahydro pyridine rings (i) we hoped to achieve this step via a Heck coupling between the alkene of the morpholine ring and 3-bromopyridine. The *N*-methylation can be carried out as previously discussed via treatment with iodomethane and sodium borohydride reduction (iii). Finally, the amide bond can be formed via reaction with 4-methylbenzoyl chloride.

This synthetic strategy offers a novel route to **1** from commercially available starting materials in six synthetic steps (Scheme 2.11).

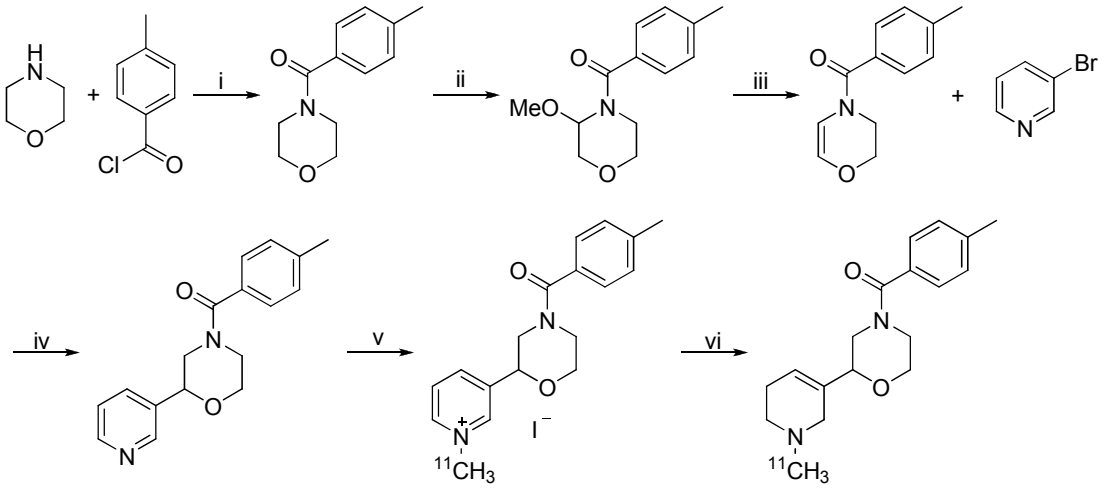

Reagents: (i) TEA, DCM (ii) NBS, HCOOH, MeOH (iii) TfOH, $CHCl_3$ (iv) Heck coupling, Pd catalyst, base (v) MeI, MeOH (vi) $NaBH_4$, MeOH

Scheme 2.11 Synthetic strategy towards **1**

Initially we had some success with this strategy with step (i) giving a good yield. Unfortunately step (ii) was somewhat problematic with no product isolated from the reaction mixture. The basis of the step was derived from previous work carried out by Liebner *et al.* into the synthesis of a variety of morpholine analogues.[48] This chemistry, while not identical to our application, had proved very successful in the original publication and thus we felt confident it would work in this case. However, having carried out numerous repetitions of this reaction with a variety of conditions, it was eventually decided to abandon this strategy to synthesise **1**.

Our second generation synthetic strategy involved a novel approach to PET contrast agent **1**. The RSA is given in Figure 2.12.

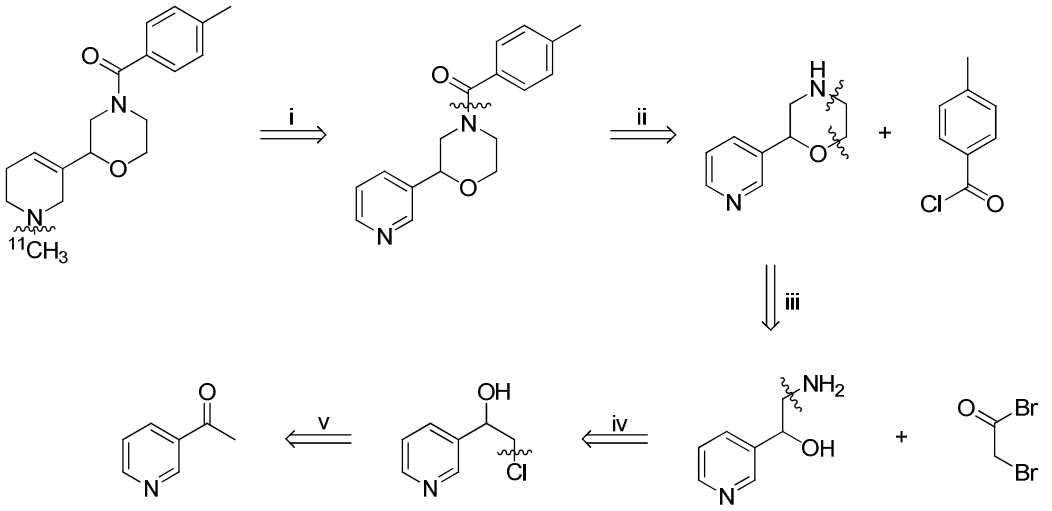

Figure 2.12 Second generation RSA towards **1**

There are distinct similarities between this revised RSA and our first attempt. Primarily, the incorporation of the radionuclide remains unchanged but the formation of the amide bond is moved later in the synthesis. To form the *C*-substituted morpholine ring we envisaged a cyclisation between an aminoalcohol and bromoacetyl bromide. The inspiration behind this step was taken from work carried out by Zindell *et al.* in 2006 into the synthesis of morpholine-derived CB2 agonists.[49] The synthetic strategy is given in Scheme 2.13.

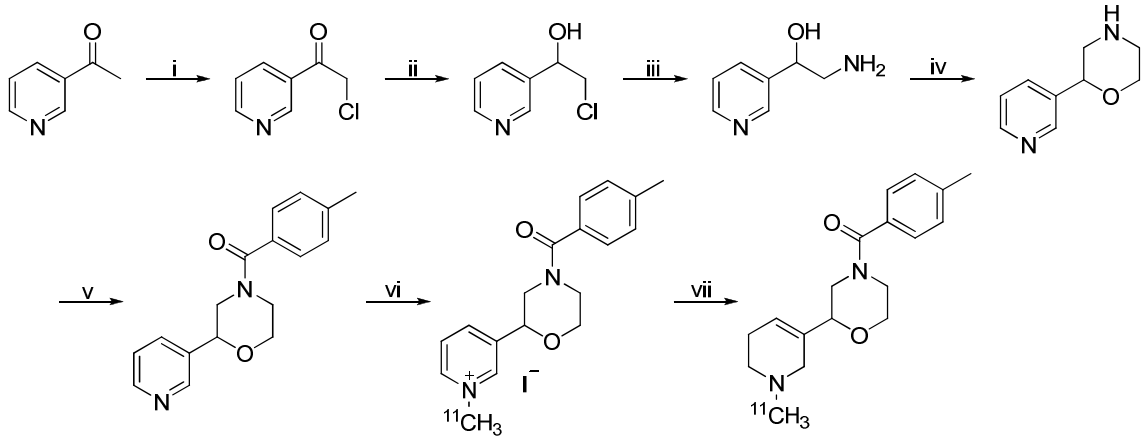

Reagents: (i) NCS, $HCl_{(g)}$, AcOH (ii) $NaBH_4$, $MeOH/H_2O$ (iii) 30% NH_4OH/MeOH then 37% HCl/EtOH (iv) a) bromoacetyl bromide, EtOAc, $NaHCO_3/H_2O$ b) KO^tBu, ^tBuOH, c) LAH, THF (v) 4-methylbenzoyl chloride, TEA, DCM (vi) MeI, MeOH (vii) $NaBH_4$, MeOH

Scheme 2.13 Second generation synthetic strategy towards **1**

Our second strategy proved much more successful with the initial steps progressing as described by Perrone *et al.* with respect to the synthesis of 3-chloroacetylpyridine, which was isolated as the hydrochloride salt. We were pleased to report an improved yield of 86% over step (i) as compared to 76% previously published by Perrone *et al.*[50] The yield of this reaction seems to be dependent on the volume of HCl gas introduced to the acetic acid. Initially we introduced HCl gas over a period of one hour as a benchmark based on the work carried out by Duquette *et al.* who reported a yield of 83% for the same reaction.[51] This did indeed give good yield in the order of 79%. However, we looked to improve on this by introducing HCl gas over an extended period of time. Introduction of HCl gas below the surface of the acetic acid over a period of two hours at 16 ^oC offered the optimum yield with 3-chloroacetyl pyridine hydrochloride crystallising out of solution in approx. 4 hours.

The following sodium borohydride reduction progressed as expected with 90% yield as a yellow oil. Purification of the crude oil by column chromatography gave the pure alcohol in 58% yield. Step (iii) proved initially problematic with respect to the isolation and purification of the amino alcohol and thus was taken as a crude mixture directly onto step (iv).

As previously stated this cyclisation was inspired by the work carried out by Zindell *et al.* with their investigation into CB2 selective agonists.[49] At our current point in the synthesis we are experiencing difficulties with the purification of the cyclised compound **B**, Figure 2.14.

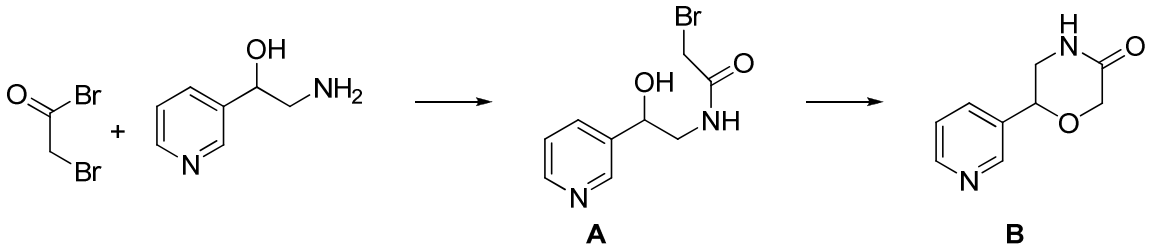

Scheme 2.14 Suggested reaction intermediates step (iv), Scheme 2.13

It is probable that the reaction proceeds in the first instance to form the amide of intermediate **A** (Scheme 2.14) under Schotten-Baumann conditions. The cyclisation to yield intermediate **B** is based-induced by deprotonation of the alcohol followed by nucleophilic substitution to displace bromide.

As discussed later, we have ceased our attempts to synthesise **1** in favour of new target compounds **2** and **3**, while access to *C*-functionalised moieties are valuable, the priority of this investigation is to demonstrate the “hot steps” for radionuclide insertion in a fully synthesised M1 muscarinic receptor compound.

CHAPTER THREE

3.0 MOLECULAR MODELLING STUDIES

Drug design is an iterative process which begins with the identification of a compound that displays an interesting biological profile and ends when both the activity profile and the chemical synthesis of the new chemical entity are optimized. Traditional approaches to drug discovery rely on a step-wise synthesis and screening program for large numbers of compounds to optimize activity profiles. Over the past ten to twenty years, scientists have used computer models of new chemical compounds to help define activity profiles, geometries and reactivities.

Over the past few years, advances in the development of new mathematical models which describe chemical phenomena and development of more intuitive program interfaces coupled with the availability of faster, smaller and affordable computer hardware have provided experimental scientists with a new set of computational tools. These tools are being successfully used, in conjunction with traditional research techniques, to examine the structural properties of existing compounds, develop and quantify a hypothesis which relates these properties to observed activity.

There are many software packages available to carry out molecular modelling, each varying in complexity and cost. In broad terms the selection of software packages can be divided into classical or quantum. The classical (or Newtonian) modelling attempts to describe a model by considering the nucleus and electrons collectively; atoms are assigned with associated mass and charge. Within a molecular model, the chemical bonds are visualised as springs considering Van der Waals forces. Electrostatic interactions are assigned based on Coulomb's law. In contrast, quantum software packages consider electrons explicitly, the benefit of classical molecular modelling is the level of complexity is reduced, thus more atoms can be considered in the model. Given the field of molecular mechanics is extensive, for the purposes of this discussion we will consider only classical molecular modelling and those techniques used within this investigation.

ENERGY MINIMISATIONS

As stated previously, in classical molecular modelling, chemical bonds are visualised as dynamic springs. When carrying out energy minimisations of a given molecule the software looks to find an energy minimum that would be representative of a molecules structure. The importance of determining a suitable starting

conformation cannot be underestimated to determine the true energy minimum for a given structure. Failure to obtain a suitable starting conformer could lead to minimisation into a local minimum where, which may not be the global minimum energy conformer. For this investigation we will carry out minimisations using a Fletcher-Powell method where by the force field constant (second derivative representative on Figure 3.0) is set to a constant and each newly generated conformer is compared to the previous derivative, the iterative process looks to achieve the desired force constant (Figure 3.0).

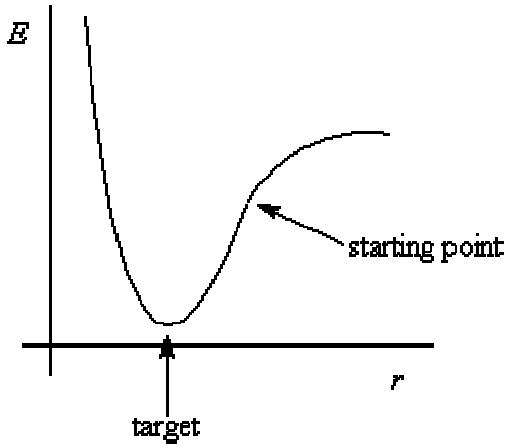

Figure 3.0 Plot of energy versus atomic radii

The major disadvantage of this process is the computational time taken, however, for small organic molecules the target force constant can generally be achieved in <500 iterations (approx. 30 minutes).

CONFORMATIONAL ANALYSIS

Once an energy minimum has been established for a given molecule, it is important to consider a range of possible conformers that could be adopted. Conformational analysis can be performed by defining rotatable bonds within a molecule at 30-360^{o} increments. The computer software compiles a spreadsheet of conformers from which the energy can be calculated, and in this case, we can carry forward the lowest energy conformers to the docking experiment. Again, the major limitation with conformational analysis is the limitation of computing power available. Clearly for increasing numbers of rotatable bonds the number of potential conformers increases exponentially. As a result, it is important to make reasonable

assumptions about the degrees of freedom around a given bond. For example, it would be unrealistic to allow the software to assess each rotatable bond in 30^{o} increments when 90^{o} increments would lead to the same energy conformer.

COMFA ANALYSIS

CoMFA (Comparative Molecular Field Analysis) is a 3D QSAR technique based on data from known active molecules. CoMFA can be applied when the 3D structure of the target receptor is unknown. To apply CoMFA, all that is needed are the activities and the 3D structures of the molecules. The aim of CoMFA is to identify a correlation between the biological activity of a set of molecules and their 3D shape, assessing their electrostatic and hydrogen bonding characteristics.

The process involves overlaying common structures and placing in a 3D grid where probe atoms are used to assess the steric and electrostatic energy (Figure 3.01), each molecule is assessed and a score is generated. These data are validated by the process of PLS (partial least squares) initially using cross validated PLS analysis, whereby one value is left out and remaining data are used in the model. This analysis is used to determine the optimal number of components to subsequently carry out non-cross validated PLS analysis. It is important to note the value of R^2 for the non-cross validated PLS analysis as this gives an indication of the predictive power of the model.

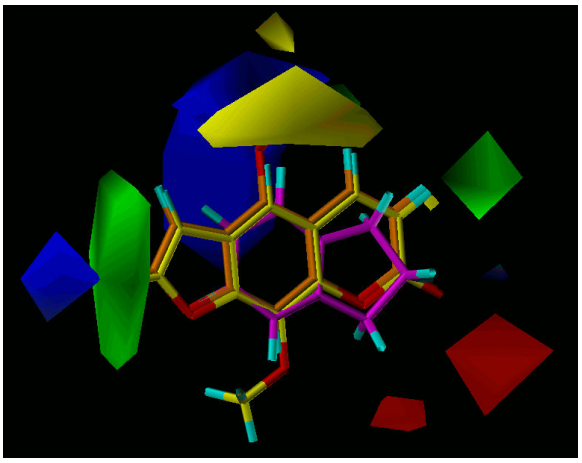

Figure 3.01 Example of overlaid structures in 3D grid

PROTEIN HOMOLOGY MODELLING

The challenge of protein modelling is one that has been addressed for many years; X-ray crystallography still remains the most powerful tool for the determination of biological macromolecule structure. However, in recent years ^{1}H NMR spectroscopy combined with computational modelling has been used to determine the structure of proteins and peptides. At present this technique is limited to use on small proteins given the complexity of these macromolecules and NMR techniques typically offer lower resolution than an X-ray diffraction structure.

There is great interest in developing techniques to model protein structures from their amino acid sequence, given that literally thousands of protein sequences are known and yet only hundreds of complete structures have been determined. However, the reasons how and why a protein folds are two crucial questions that need to be addressed before a satisfactory prediction of secondary and tertiary structures can be made. Furthermore, assuming proteins fold at random, the computational resources required to assess every possible structure and conformational state with multiple energy minima is intangible.

Protein homology modelling has thus far proved to be the most successful method for predicting a tertiary structure. The process develops a model of an unknown protein structure from a known structure of homologous protein. The success of the procedure is based on the fact that protein secondary structures are well conserved between homologous proteins.

In the first instance, the two amino acid sequences are compared to identify areas of agreement. Particularly, we look for agreement between the two primary structures at critical areas in the sequence, namely, the active site, helices and β sheets. The primary sequence can be modified if required to ensure good alignment between the two sequences, however, amino acid substitutions are generally not extensive since protein function is not dependant on one residue and mutations on the exterior of the protein do not inhibit protein function.

Once a suitable model has been identified, the unknown protein structure is superimposed on the one that is known and by computational analysis the model is generated. It is worth noting that any suggested model should be scrupulously examined for key features such as di-sulfide bridges to ensure good agreement with that of the original model.

3.1 RESULTS AND DISCUSSION

As part of our particular interest in M1 muscarinic receptor we sought to construct a model of the M1 muscarinic receptor and perform docking studies with a range of compounds based on those evaluated *in vitro* by Augelli-Szafran *et al*.[3] By collaboration within the Interreg group we were able to gain access to the necessary software working under the supervision of Prof. R. Bureau (CERMN, Uni Caen). Within this collaboration our aim was to carry out protein modelling, docking studies and gain familiarity with the Tripos-Sybyl X software package that had currently not been used to carry out such an investigation. We aim to identify key residues within the M1 muscarinic receptor that will lead to a more targeted approach to the design of M1 muscarinic receptor antagonists. Furthermore, given the advances that have been made in the field of molecular mechanics in the past 5 years, we look to validate our data against *in vitro* data obtained by Augelli-Szafran *et al*.[3]

In the first instance, we identified a range of analogues, from those synthesised by Augelli-Szafran to represent the range of binding results, previously determined, on which we could carry out the modelling. These analogues had a range of IC_{50} values varying from nano to micro molar, identified in Table 3.0 with their respective IC_{50} value towards the M1 muscarinic receptor. It is important to note that in the original publication by Augelli-Szafran, *et al.* No consideration was given to the absolute stereochemistry between motifs R and S (Figure 3.02); however for our purposes we modelled both the R and S forms to determine any discrepancies in predicted binding affinities between the two isomers.

Once we identified these range of analogues we set about modelling our database using the program Sybyl X. This process involved the construction of each analogue by overlaying each analogue with a known crystal structure of similar pharmacophore, namely the di-substituted tetrahydropyridine ring. These analogues were then subject to minimisation techniques to identify local energy minima using a Powell method with a gradient termination value of 0.05 kcal/mol. The Tripos force field was considered given we are considering small organic molecules, no consideration was given to charge.

The subsequent energy minimised analogues were processed to generate a range of conformers (in the order of 100-200 conformers) using a systematic search.

This process involves identifying rotational bonds within each analogue and specifying the degrees of freedom around each bond. For example the degree of rotation around the ester is 180 degrees, whereas the degree of freedom around C-C bond is 360 degrees in 30 degree increments. This is a limitation of the software as it will only assess rotational bonds in 30 degree increments. Another important consideration when undertaking any molecular modelling experiment is to assess the computational capacity available given this will determine the range of conformers that can be processed. In this case we felt anything up to 200 conformers of each analogue would be a good representation to allow successful analysis. For this selection of conformers the relative conformational energy was calculated. One such example is given in Figure 3.03.

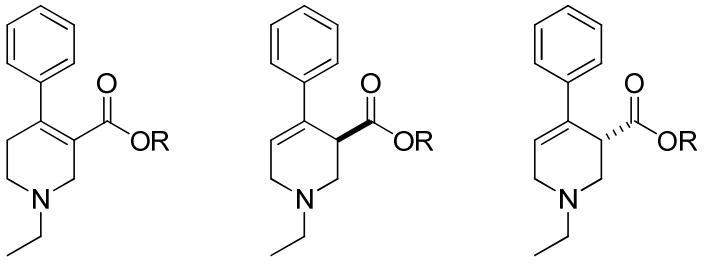

A **B (R)** **B (S)**

Figure 3.02 Structural motifs of pharmacophore

Compound	Motif	Isomer	R	IC_{50} (nM)
4	B	R	$(CH_2)_5CH_3$	27.3
5	B	S	$(CH_2)_5CH_3$	27.3
6	A	-	$CH_2C_6H_{11}$	14.5
7	A	-	C_6H_{11}	18.1
8	B	R	C_6H_{11}	16.9
9	B	S	C_6H_{11}	16.9
10	A	-	$(CH_2)_2Ph$	9.6
11	A	-	$CH_2CH(CH_3)_2$	120.5
12	B	R	$CH_2CH(CH_3)_2$	128
13	B	S	$CH_2CH(CH_3)_2$	128
14	A	-	$(CH_2)_9CH_3$	106.1
15	B	R	$(CH_2)_2Ph$-*p*-OCH_3	159
16	B	S	$(CH_2)_2Ph$-*p*-OCH_3	159

17	A	-	CH_3	2308
18	B	R	CH_3	33117
19	B	S	CH_3	33117
20	A	-	Ph	1819
21	A	-	CH_2CH_3	888
22	A	-	$(CH_2)_2$Ph-*p*-OCH_3	1941

Table 3.0 Range of analogues identified for modelling study

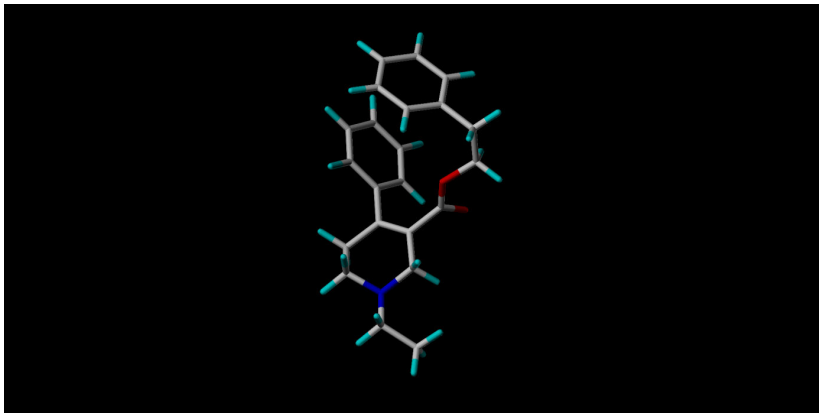

Figure 3.03 Lowest energy state of compound **10** following conformational analysis

The example given in Figure 3.03 is a typical result of the conformational analysis performed with an energetically stable conformation adopted as a result of structural characteristics. Namely, this class of molecules adopt a folded conformation to stabilise Van der Waals forces between the R group and the substituted aromatic of the tetrahydropyridine ring. In Figure 3.03 we see the two aromatic rings arranging themselves in as close to a stacked position as conformationally possible given the defined bond rotations. In other alkyl R substituted examples this folding is mirrored, this may not be truly representative of the conformation the substrate would adopt *in vivo*, but is a reasonable estimation given hydrophobic nature of the alkyl/aromatic groups in aqueous solution. Unsurprisingly, the *N*-ethyl group adopts an equatorial position on the twist-boat of the tetrahydropyridine ring, minimising 1-3 steric interactions.

Figure 3.04 shows an example of compounds **18** and **19**. When compared to the compound **10** in Figure 3.03 we see structural similarities with respect to the

folding of the R group across the aromatic ring, but also structural differences in that the tetrahydropyridine ring is flipped. However, the *N*-ethyl maintains its equatorial position for the reason previously stated.

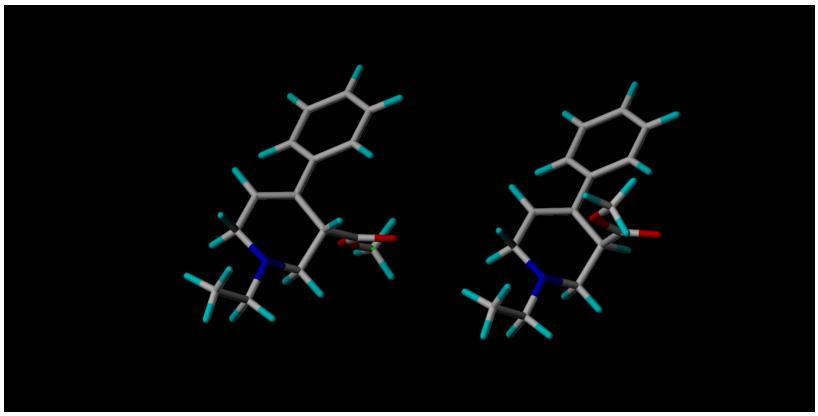

Figure 3.04 Lowest energy state of compounds **18** (right) and **19** (left) following conformational analysis

From the database of conformers, the energy for each conformer was calculated and the lowest energy conformer selected to take forward to the docking study (Appendix 1). The docked conformers were subject to COMFA analysis and the results treated by PLS statistical analysis to determine the validity of the results (Figure 3.06). The results from PLS analysis carrying out non-cross validation across 19 components yielded a value of R^2 = 0.457. This is regarded as a good correlation between predicted and experimental binding affinity (R^2 > 0.5 – excellent correlation).

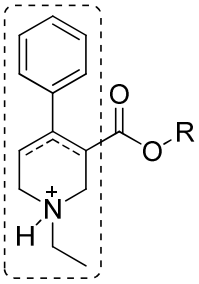

Figure 3.05 Identified pharmacophore for COMFA analysis

Compound	Motif	Isomer	COMFA Score	IC_{50} (nM)
4	B	R	81	27.3
5	B	S	82	27.3

6	A	-	80	14.5
7	A	-	78	18.1
8	B	R	77	16.9
9	B	S	75	16.9
10	A	-	82	9.6
11	A	-	73	120.5
12	B	R	67	128
13	B	S	68	128
14	A	-	94	106.1
15	B	R	86	159
16	B	S	83	159
17	A	-	61	2308
18	B	R	62	33117
19	B	S	60	33117
20	A	-	71	1819
21	A	-	65	888
22	A	-	83	1941

Table 3.01 Summary of results from COMFA analysis

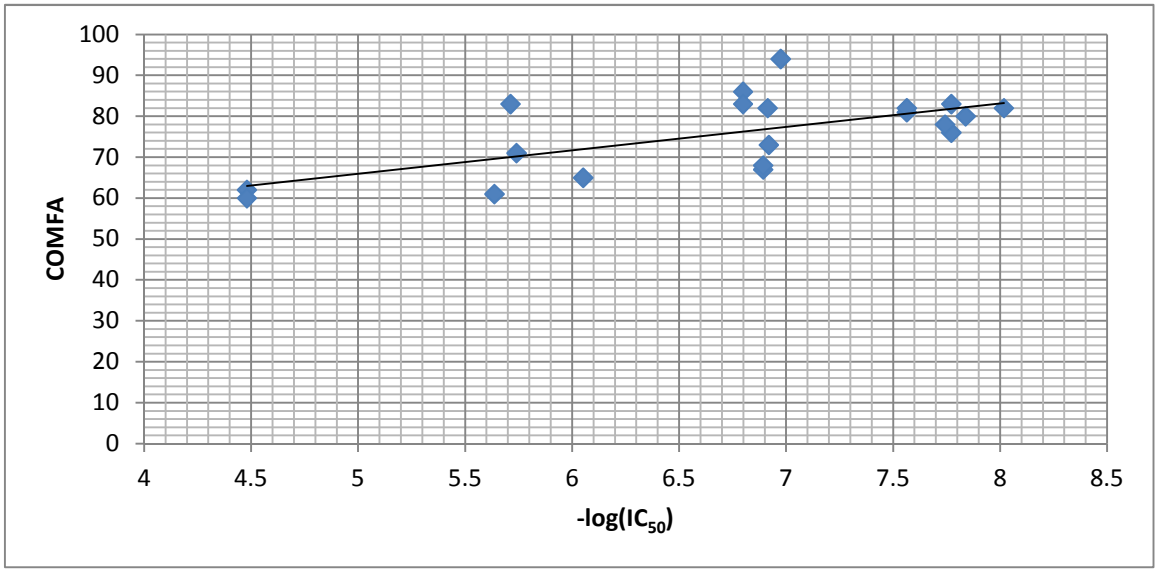

Figure 3.06 Plot of experimentally determined IC_{50} binding affinity versus predicted score (COMFA analysis) (R^2 = 0.42)

With an extensive database of conformers in hand we set about modelling the M1 muscarinic receptor to carry out the docking experiment. The crystal structure of the M1 muscarinic receptor has not been published to date. As a result we had to construct our model based on known crystal structures of similar proteins. By sequential analysis, using information from the protein data bank we found a 95% agreement in the primary structure of M1 muscarinic and β2 adrenergic receptor. Following sequence alignment (Appendix 2) between the human M1 muscarinic and β2 adrenergic receptor we observe good agreement on all 7 helices, as a result we were able to superimpose the M1 muscarinic receptor primary sequence onto the crystal structure of antagonist bound human β2 adrenergic receptor (Figure 3.07) to yield the predicted structure of M1 muscarinic receptor (Figure 3.08). On close examination we see good correlation in the secondary structure and importantly in tertiary structure with disulfide bridges conserved between models.

Figure 3.07 Antagonist bound β2 adrenergic receptor

Note the presence of additional structure positioned intracellular to the receptor (bottom of picture), this was necessary to obtain a crystal structure of β2 adrenergic receptor and thus must be included in the model of M1 muscarinic receptor. This is an acceptable modification as it does not impede the ligands binding which occurs on the extracellular face of the receptor. With a model in hand we turned our attention to carrying out the docking experiment of our conformers

with the M1 muscarinic receptor. The results for the most tightly bound conformer of each analogue is summarised in Table 3.02.

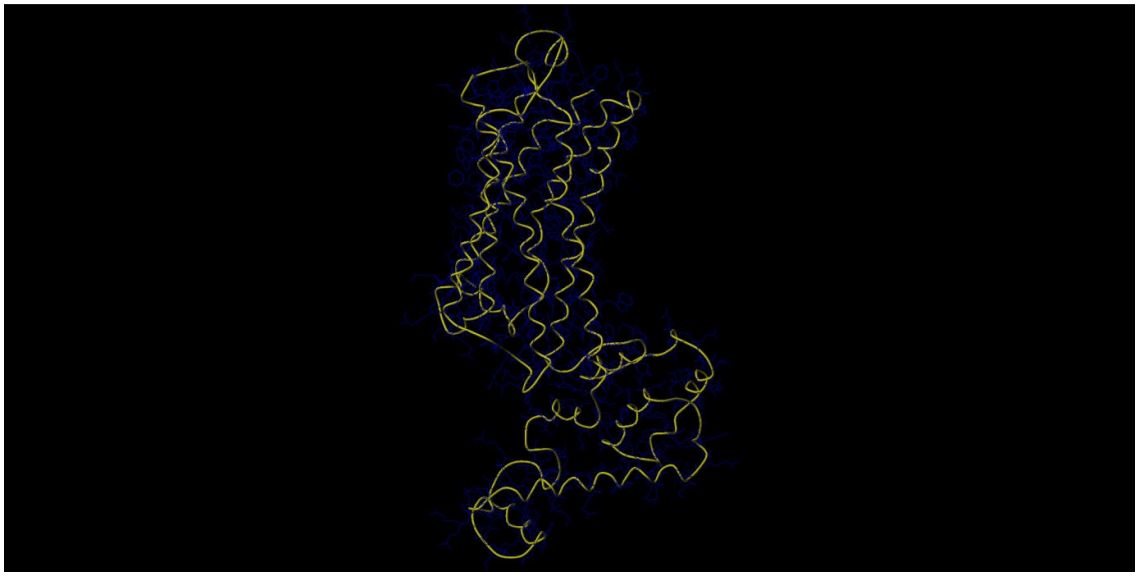

Figure 3.08 Predicted M1 muscarinic receptor tertiary structure

Compound	Motif	Isomer	COMFA Score	IC_{50} (nM)	Binding Score*
4	B	R	81	27.3	5.04
5	B	S	82	27.3	4.34
6	A	-	80	14.5	6.84
7	A	-	78	18.1	4.46
8	B	R	77	16.9	-‡
9	B	S	75	16.9	-‡
10	A	-	82	9.6	5.12
11	A	-	73	120.5	4.53
12	B	R	67	128	4.23
13	B	S	68	128	3.61
14	A	-	94	106.1	5.45
15	B	R	86	159	3.81
16	B	S	83	159	5.64
17	A	-	61	2308	2.48
18	B	R	62	33117	3.53
19	B	S	60	33117	2.65

20	A	-	71	1819	3.94
21	A	-	65	888	3.93
22	A	-	83	1941	4.88

*Score generated from Surflex-Dock (SFXC) methodology ‡Compounds **8** and **9** were rejected from the docking study due to steric clash with protein residue.

Table 3.02 Summary of results from docking experiment

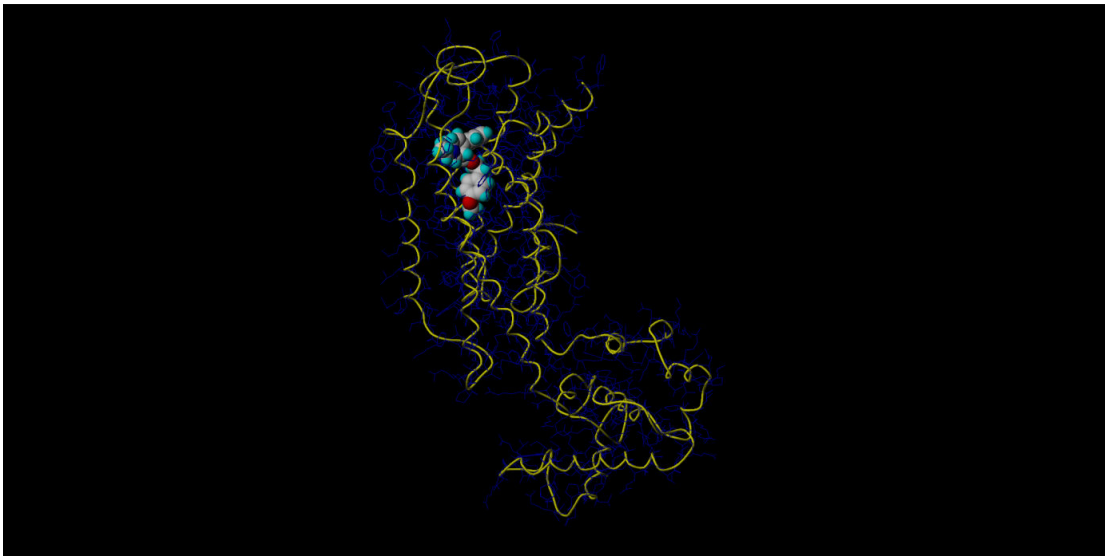

Figure 3.09 M1muscarinic receptor showing protomol for docking study (Appendix 2)

Thus far we have determined that electrostatic interactions between the quaternary amine and aspartic acid (ASP 105) combined with hydrogen bonding between the proton of the quaternary amine and tyrosine (TYR 404) are responsible for the binding of our analogues to the M1 receptor. There are hydrophobic pockets for the dihydropyridine substituted aromatic and the various R functionalities that are all alkyl or aromatic.

The binding position of the dihydropyridine ring and the substituted aromatic are well conserved across the analogues assessed. However, while the R groups adopt similar positions in the hydrophobic pocket, their relative size appears to have a direct impact on the hydrogen bonding and electrostatic distance between the quaternary amine and the receptor. This would account for the variation in IC_{50} values observed *in vitro*, given there is correlation between predicted binding affinity and experimentally determined affinity. A plot of the binding score versus *in vitro*

(Figure 3.11) shows moderate agreement between the computationally determined binding score and *in vitro* IC_{50} values with R^2 = 0.310. The reason for the lack of agreement is likely in part due to our modelling of both the R and S isomers since their respective binding scores are plotted against the same IC_{50} value. These IC_{50} values were determined with a racemic mixture of the isomers when in fact we predict, unsurprisingly, their binding interactions are very different.

In summary, we have constructed a suitable model of M1 muscarinic receptor and through docking studies have shown good agreement with *in vitro* data. Furthermore, we have identified key structural features that are crucial for M1 binding that offer new insight to further develop M1 selective compounds.

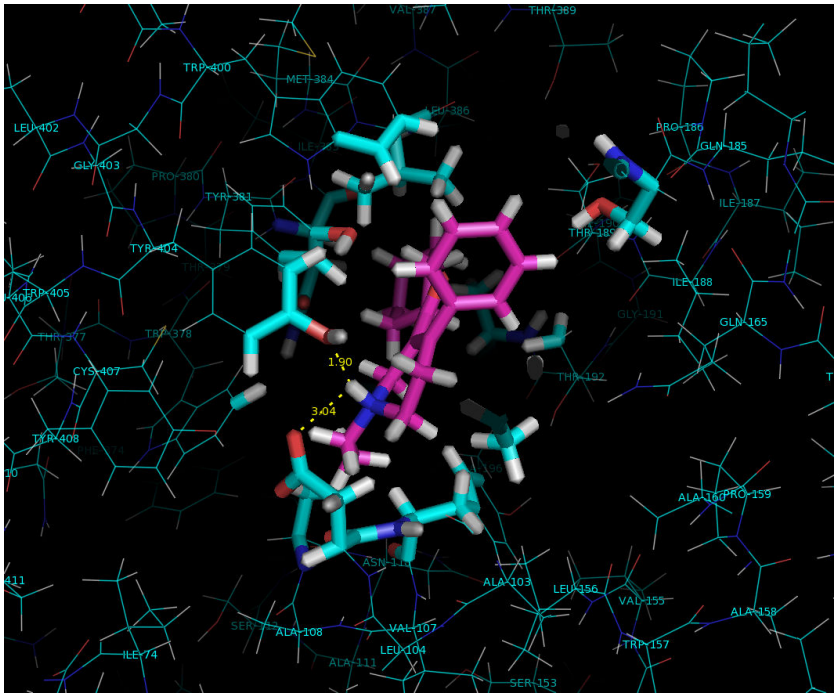

Figure 3.10 Compound **7** docked into receptor – hydrogen bonding and electrostatic interactions shown

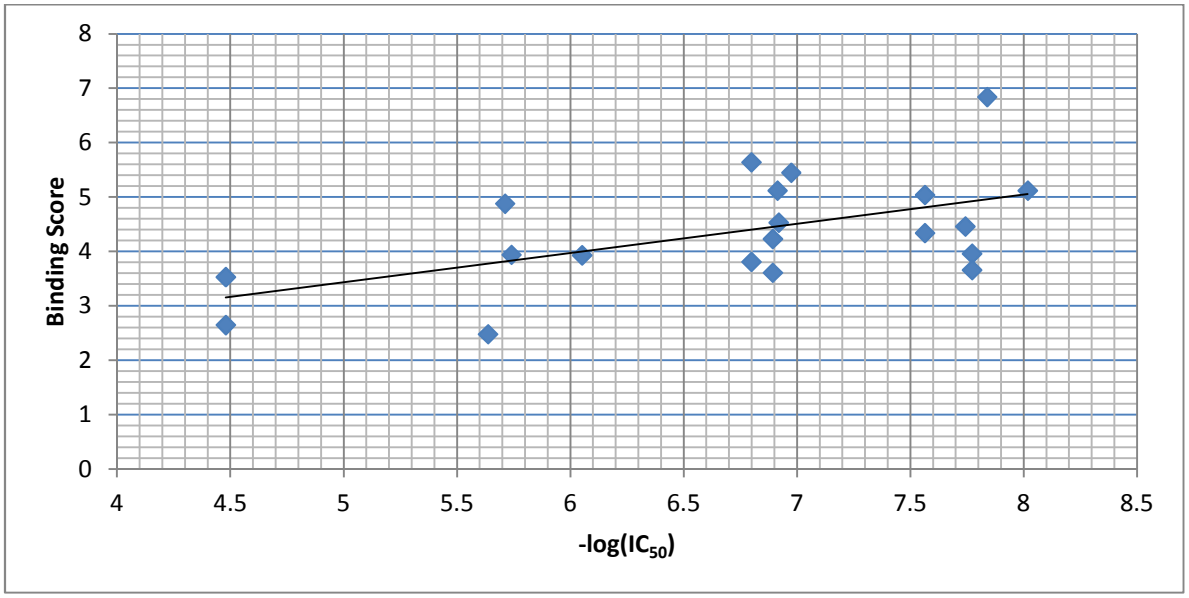

Figure 3.11 Plot of experimentally determined IC_{50} binding affinity versus predicted score (docking analysis) (R^2 = 0.310)

CHAPTER FOUR

4.0 TOWARDS THE SYNTHESIS OF 2 AND 3

As previously stated this work has been carried out in collaboration with Dr. Cécile Perrio (Laboratoire de Développements Méthodologiques en TEP, Cyceron) who has offered invaluable advice with respect to the current methodologies employed in the synthesis of PET contrast agents. After reviewing our work in the synthesis of **1**, we were given the advice that a M1 muscarinic receptor antagonist would be of greater value than the agonist.

Given our work to date has looked to employ the incorporation of ^{11}C radiolabel at an *N*-alkyl position we propose to find a suitable M1 muscarinic receptor antagonist that could follow in this theme. After an extensive literature search we were pleased to identify our second target molecule (Figure 4.0) from the work carried out by Augelli-Szafran *et al* in 1999.[3] This was an attractive publication as it details the synthesis of a wide range of molecules that had been assessed *in vitro* for SAR for all 5 muscarinic receptor sub-types.[3]

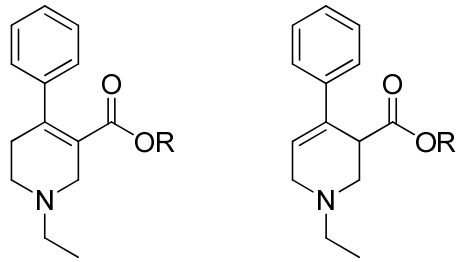

A **B**

Figure 4.0 1, 4-Disubstituted tetrahydropyridine motifs

In the same way as our previous work, the two compounds **A** and **B** are synthesised from pyridine derived starting materials and the *N*-ethyl group introduced at the end of the synthesis followed by $NaBH_4$ reduction (Scheme 4.0).

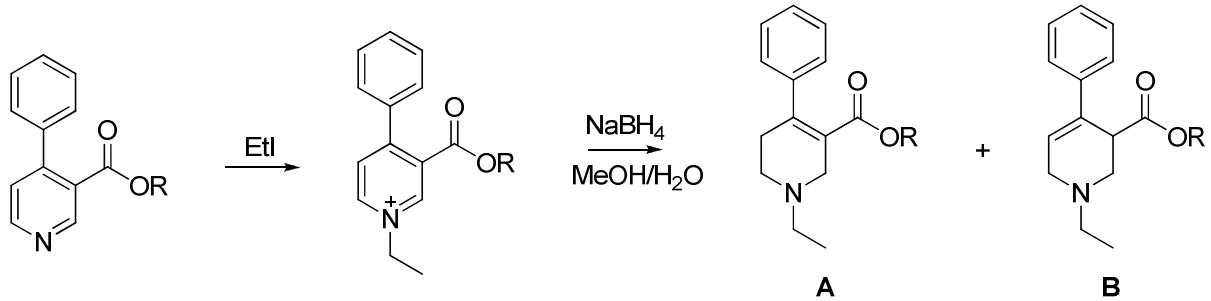

A **B**

Scheme 4.0 *N*-ethylation and $NaBH_4$ reduction to yield **A** and **B**

This compliments our work to date with the added synthetic challenge of yielding two regio-isomers from the reduction step.

We quickly identified a suitable target compound that had a high affinity (nM) and specificity for M1 muscarinic receptor (Figure 4.01).

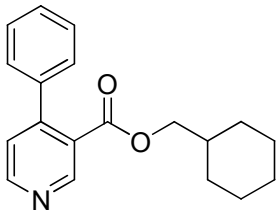

Figure 4.01 Target precursor prior to radiolabel introduction

We looked to synthesise a good quantity of the precursor (Figure 4.01) that could then be tested to develop the rapid reactions to incorporate a suitable radiolabel (Scheme 4.01).

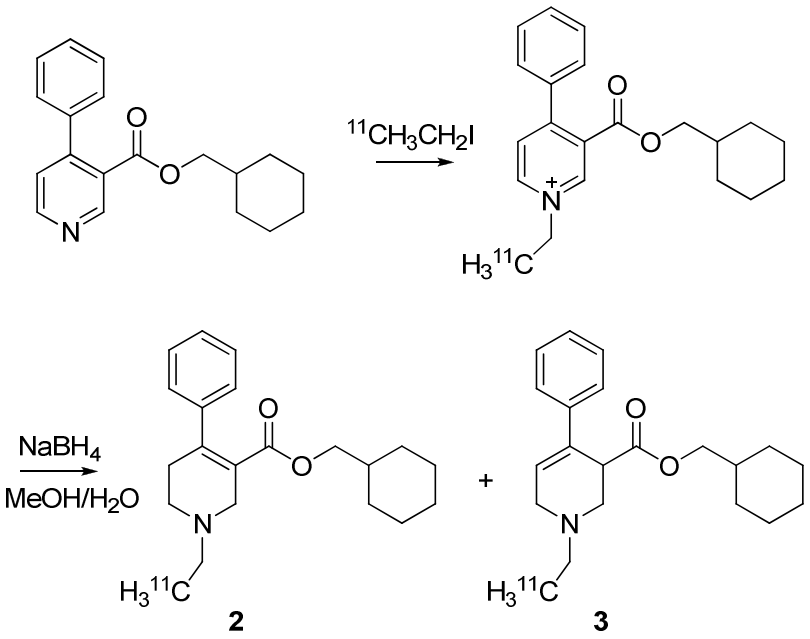

Scheme 4.01 Synthetic strategy to ^{11}C labelled muscarinic receptor antagonist

In the work published by Augelli-Szafran *et al.* they offer a suitable synthetic strategy to the target compounds **2** and **3**.[3] Thus, we planned to carry out the same synthetic procedures (Scheme 4.02) to afford **2** and **3**. Compound **3** exhibits high affinity for M1 muscarinic receptor with nano molar concentrations, as well as high specificity for the M1 subtype with respective affinities for M2-M5 subtypes at 10^2 fold higher concentrations.

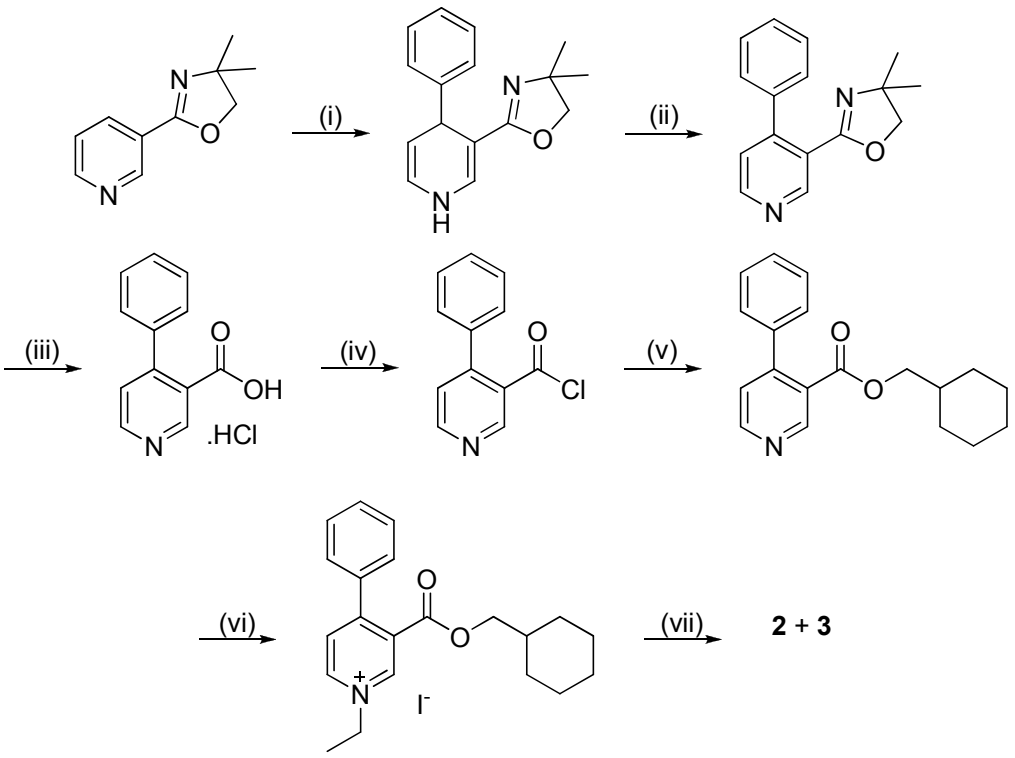

(i) PhLi, THF, -78 ^{o}C (ii) S_8, Δ, $PhCH_3$ (iii) conc. HCl, Δ (iv) $SOCl_2$, Δ (v) cyclohexylmethanol, DCM, Et_3N, 0 ^{o}C to r.t. (vi) EtI, Δ (vii) $NaBH_4$, MeOH/H_2O.

Scheme 4.02 Synthetic strategy to **2** and **3**

Note: While we propose the incorporation of ^{11}C label, in practice we carry out the synthesis with ^{12}C to demonstrate the required chemistry.

Our first synthetic challenge was to synthesise 4,4-dimethyl-2-(pyridin-3-yl)-4,5-dihydrooxazole prior to carrying out the synthesis described by Augelli-Szafran *et al*. Our initial strategy (Scheme 4.03) while successful, did not give a satisfactory yield in the final cyclisation to afford the oxazoline.

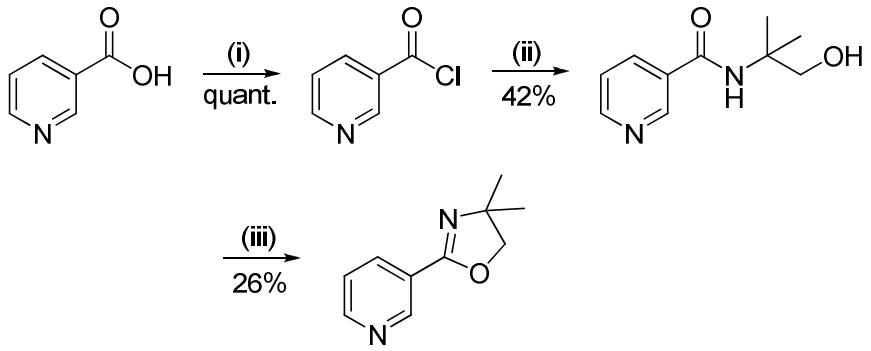

(i) $SOCl_3$, Δ (ii) 2-amino-2-methylpropan-1-ol, Et_3N, 0 ^{o}C to r.t (iii) $SOCl_2$, r.t.

Scheme 4.03 Synthesis of oxazoline precursor

At this point a literature search yielded a solution from the work carried out by Vorbrüggen and Krolikiewicz in 1993 which synthesised the desired oxazoline from nicotinic acid in one step (Scheme 4.04) by employing the Appel reaction in good yield.[52]

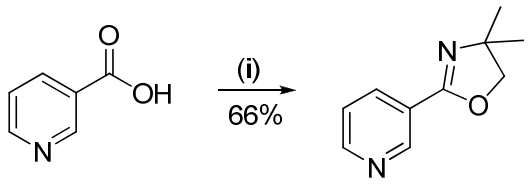

(i) PPh_3, 2-amino-2-methylpropan-1-ol, Et_3N, CCl_4, MeCN, 0 ^oC to r.t, 24 hrs.

Figure 4.04 Appel reaction of nicotinic acid to afford the desired oxazoline.

Our complete synthetic strategy is given in Figure 4.05 affording a mixture of **2** and **3** from nicotinic acid.

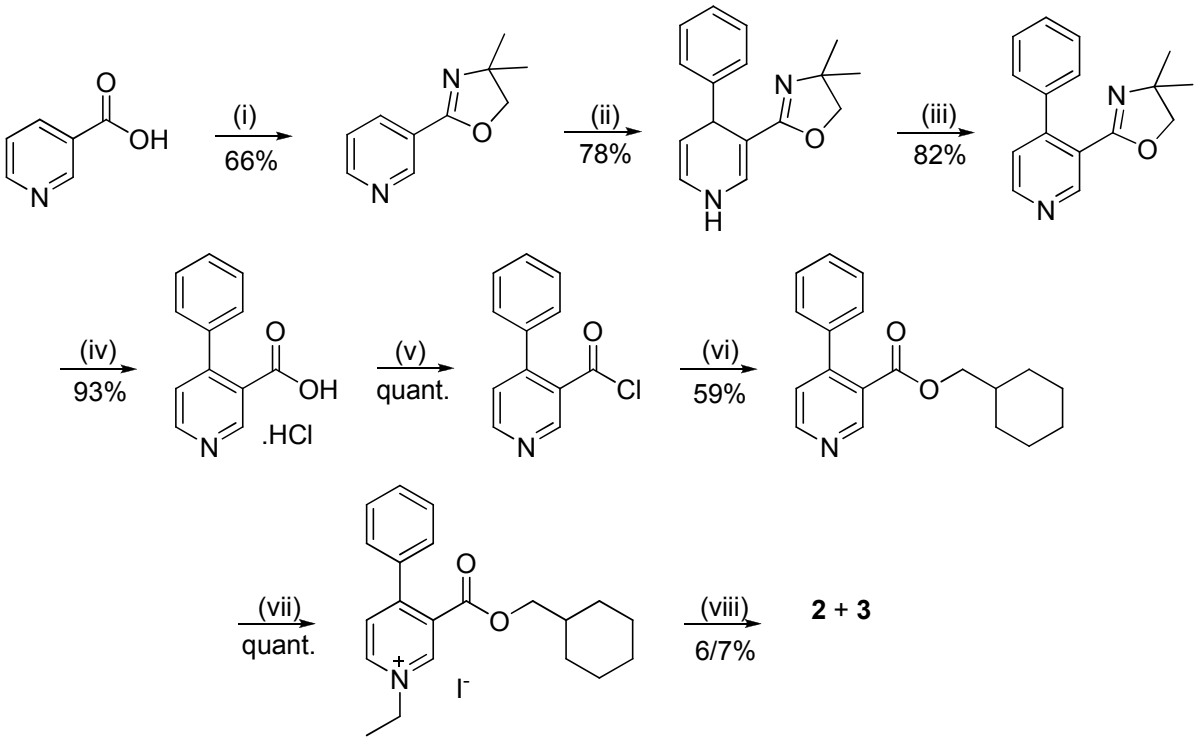

(i) PPh_3, 2-amino-2-methylpropan-1-ol, Et_3N, CCl_4, MeCN, 0 ^oC to r.t. (ii) PhLi, THF, -78 ^oC (iii) S_8, Δ, $PhCH_3$ (iv) conc. HCl, Δ (v) $SOCl_2$, Δ (vi) cyclohexylmethanol, DCM, Et_3N, 0 ^oC to r.t. (vii) EtI, Δ (viii) $NaBH_4$, $MeOH/H_2O$, Δ.

Figure 4.05 Complete synthetic strategy to **2** and **3**.

We are pleased to report the syntheses of **2** and **3** utilising a robust and reproducible synthetic protocol. Having carried out the syntheses of **2** and **3** without considering

the time restrictions of the *N*-ethylation and sodium borohydride reductions we have achieved similar yields to that reported by Augelli-Szafran *et al*.

Following this we attempted the “hot steps” as could be performed in the synthesis of a PET contrast agent with ^{11}C. Again, we are pleased to report this was carried out in glassware with 18% and 5% yields for *N*-ethylation and reduction respectively. While the reactions can be carried out in acceptable yields given the time constraints we have yet to demonstrate a purification protocol to yield **2** and **3**.

CHAPTER FIVE

5.0 CONCLUSION

M1 MUSCARINIC RECEPTOR AGONIST 1

Having carried out kinetic studies into the *N*-methylation and regio-selective reduction of pyridine and isoquinoline models we felt these models studies were transferable to the target compound **1**. Despite the difficulties with a novel synthetic route to **1** in the first instance, we are confident that we will be able to fully synthesise **1** by our second synthetic strategy and hope to complete this work to demonstrate accessibility to a range of *C*-functionalised morpholine moieties.

By demonstrating our "hot step" protocol, we hope to transfer our findings to new examples of M_1 muscarinic receptor antagonists. It is hoped this will add to our understanding of the M_1 muscarinic receptor and ultimately allow the development of highly specific M_1 muscarinic receptor agonists/antagonists. By characterising these receptors using PET we would hope suitable targets can be identified for development to a viable treatment to slow the progression of AD.

M1 MUSCARINIC RECEPTOR ANTAGONIST 2 AND 3

Having demonstrated the synthesis of **2** and **3** in glassware in yields acceptable to the application of PET imaging we are looking to develop a robust purification protocol. As a result we have turned our attention to offering a HPLC (high performance liquid chromatography) protocol to yield **2** and **3**. Currently our work has showed good promise with the racemic mixture of **2** and **3** separable on reverse-phase HPLC (HPLC conditions: Hi Chrom C_{18}, 4.6 x 150 mm, MeOH:H_2O:0.01% TEA, 0.5 mL/min; 10 min). Elution times vary between 3 – 6 min for compounds **2** and **3**. We are currently optimising the conditions to separate **2** and **3** in a reproducible manner.

In the future we look to not only offer a process of separation of **2** and **3**, but also the separation of the two enantiomers of **3** by employing a Diacel ChiralPak OD column. This would allow *in vitro* assays to be carried out on both the R and S forms of **3**.

Aside from this work we are looking to carry out the borohydride reduction in flow with the HPLC purification. This is carried out with polymer supported borohydride packed into a 100 mm HPLC column. Currently we have achieved the required reduction; however, the current yield is < 1%. To address this issue we plan to employ the use of a column oven to achieve greater yield. Once this process

has been refined we will be able to offer the reduction and purification in < 10 min. This would constitute a significant step forward and a viable method for introducing ^{11}C radiolabels into similar compounds. We plan to develop this process for both *N*-methyl and *N*-ethyl series of our compounds.

While this work was carried out, the efficient *N*-methylation and borohydride reduction with the use of ^{11}C methyliodide has been published by our partners in Caen. While this was disappointing we are confident that by developing our protocol onto a flow system we can add value to the work already carried out by Gourand *et al.*[53]

CHAPTER SIX

6.0 EXPERIMENTAL

Thin layer chromatography was carried out on aluminium-backed plates coated with 0.25 mm Merck Kiesel 60 F254 silica gel. The plates were visualised by ultra violet irradiation at a wavelength of 254 nm. Flash chromatography was carried out using Merck Kiesel gel 60 (70-230 mesh).

Infrared spectra were carried out using Perkin-Elmer Paragon 1000 FT-IR spectrophotometer in the range of 4000-600 cm^{-1}. Samples were dissolved in an appropriate solvent and applied to sodium plates as thin films. In the case of liquid samples, they were applied neat as a thin film on sodium plates. Only major absorbances have been quoted.

^{1}H-NMR and ^{13}C-NMR spectra were measured using either a Varian Gemini 300 MHz spectrometer or Varian Lambda 400 MHz spectrometer. The solvent used is stated using TMS (trimethylsilane) as the internal standard.

The following references have been used in the description of NMR spectra: δ = chemical shift (in ppm), *J* = coupling constant (in Hz), s = singlet, br s = broad singlet, d = doublet, dd = double doublet, dt = double triplet, dq = doublet quartet, t = triplet, m = multiplet, C_q = quaternary carbon determined by DEPT.

Melting points were obtained using an Büchi B-545 melting point instrument and are uncorrected.

Unless otherwise stated all chemicals of reagent grade were obtained from Sigma-Aldrich.

NMR studies into *N*-methylation of pyridine

Pyridine-d_5 (0.15 mL, 2 mmol) and iodomethane (0.1 mL, 1.6 mmol) was added to MeOD (0.45 mL) in a NMR tube. The ^{1}H NMR spectra (300 MHz) were monitored every two minutes for an eight minute period in total (Figure 2.08). Care was taken in the use of MeOD outside of fume hood.

Preparation of 1-methylpyridinium iodide – 2 hours[54]

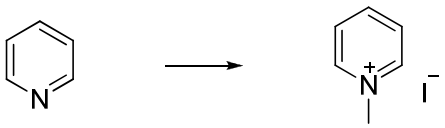

Pyridine (4.5 mL, 4.7 g, 0.06 mol) in methanol (35 mL) was added to a round bottomed flask fitted with condenser, drying tube and pressure-equalising dropping

funnel. The dropping funnel was charged with iodomethane (3.1 mL, 7.1 g, 0.05 mol) and added dropwise (*c.a* 5 min). The reaction mixture was stirred at room temperature for two hours. Solvent was removed *in vacuo*, the yellow crystalline solid washed with diethyl ether and dried *in vacuo* to yield the title compound (9.34 g, 62%); m.p. 113.1 ^{o}C (lit. 116-117 ^{o}C); IR ν_{max} (DCM)/cm^{-1} 3037 (C-H alkene), 1631 (C=C alkene), 1484 (C-H alkane), 1285 (C-N amine), 764 (C-H alkene); ^{1}H NMR (400 MHz, $CDCl_3$) δ 9.17 (2 H, d, *J* = 8.0, C**H**$_A$Ar), 8.42 (1 H, t, *J* = 8.0, C**H**$_C$Ar), 8.04 (2 H, t, *J* = 8.0, C**H**$_B$Ar), 4.66 (3 H, s, C**H**$_3$); ^{13}C NMR (75 MHz, $CDCl_3$) δ 146.2 (**C**H Ar), 145.1 (**C**H Ar), 48 (**C**H$_3$).

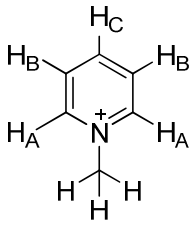

^{1}H NMR assignments

General procedure for the preparation of 1-methylpyridinium iodide – 3 mins[54]

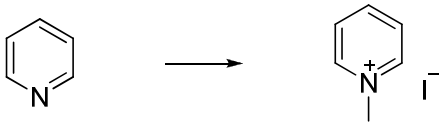

Pyridine (4.5 mL, 4.7 g, 0.06 mol) in methanol (35 mL) was added to a round bottomed flask fitted with condenser, drying tube and heated to required temperature (Table 5.0). Iodomethane (3.1 mL, 7.1 g, 0.05 mol) was added and the reaction stirred at a set temperature for three minutes. Solvent was removed *in vacuo*, the yellow crystalline solid washed with diethyl ether and dried *in vacuo* to yield the title compound in its respective yield (Table 6.0).

Time (min)	Temperature (^{o}C)	Concentration of pyridine (mol)	Concentration of MeI (mol)	Yield of **2** (% from pyridine)
120	25	0.06	0.05	62%
3	30	0.06	0.05	nil
3	35	0.06	0.05	nil
3	40	0.06	0.05	4%
3	45	0.06	0.05	7%

3	50	0.06	0.05	8%
3	55	0.06	0.05	10%
3	60	0.06	0.05	14%
3	reflux	0.06	0.05	16%

Table 6.0 Kinetic studies for *N*-methylation of pyridine

Preparation of 2-methylisoquinolinium iodide[54]

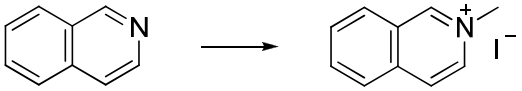

Isoquinoline (7.11 mL, 7.75 g, 0.06 mol) in methanol (35 mL) was added to a round bottomed flask fitted with condenser, drying tube and pressure equalising dropping funnel. The dropping funnel was charged with iodomethane (3.1 mL, 7.1 g, 0.05 mol) and added dropwise (*c.a* 10 min). The reaction mixture was stirred at room temperature for two hours. Solvent was removed *in vacuo*, the yellow crystalline solid washed with diethyl ether and dried *in vacuo* to yield the title compound (11.49 g, 85%); m.p 159.9-161.1 ^{o}C (lit. 160-162 ^{o}C); IR ν_{max} (DCM)/cm^{-1} 3062 (C-H alkene), 2961 (C-H alkane), 1649 (C-H phenyl), 1605 (C=C Ar), 1391 (C-H alkane), 1178 (C-N amine), 811 (C-H phenyl), 756 (C-H phenyl); ^{1}H NMR (300 MHz, $CDCl_3$) δ 10.71 (1H, s, C**H**$_G$Ar), 8.74 (1H, dd, *J* = 8.4, 1.2, C**H**$_B$Ar), 8.64 (1H, d, *J* = 8.4, C**H**$_A$Ar), 8.37 (1H, d, *J* = 6.6, C**H**$_F$Ar), 8.13 (1H, dd, *J* = 6.6, 1.2, C**H**$_E$Ar), 8.08 (1H, dd, *J* = 6.6, 1.2, C**H**$_D$Ar), 7.91 (1H, dd, *J* = 6.6, 1.5, C**H**$_C$Ar), 4.73 (3H, s, C**H**$_3$); ^{13}C NMR (75 MHz, $CDCl_3$) δ 150.9 (**C**H Ar), 137.3 (**C**H Ar), 136.3 (**C**H Ar), 131.0 (**C**H Ar), 130.2 (**C**H Ar), 127.5 (**C**H Ar), 127.0 (**C**H Ar), 125.0 (**C**H Ar), 120.0 (**C**H Ar), 48.6 (**C**H$_3$).

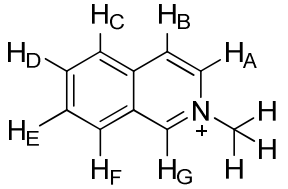

^{1}H NMR assignments

Preparation of 2-methyl-1,2,3,4-tetrahydroisoquinoline – 20 mins[55]

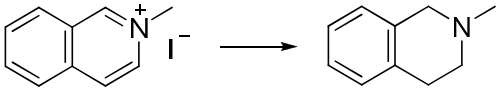

2-Methyl isoquinolinium iodide (3 g, 0.021 mol) in methanol (20 mL) and water (10 mL) was cooled to 0 °C. Sodium borohydride (3 g, 0.072 mol) was added in portions (*c.a* 5 mins) then rapidly heated to reflux for 15 mins. Once cooled the reaction mixture was washed with a saturated aqueous solution of ammonium chloride and extracted into diethyl ether. Concentration *in vacuo* and purification by distillation afforded the title compound as a colourless oil (1.60 g, 52%); b.p 88 °C (11 mbar); IR ν_{max} (DCM)/cm^{-1} 3055 (C-H alkene), 2971 (C-H alkane), 1610 (C=C Ar), 1380 (C-H alkane), 1178 (C-N amine); ^{1}H NMR (300 MHz, $CDCl_3$) δ 7.53 (1H, d, *J* = 7.2, C**H**$_C$Ar), 7.45 (1H, dd, *J* = 7.2, 3.0, C**H**$_D$Ar), 7.20 (1H, dd, *J* = 7.2, 2.8, C**H**$_E$Ar), 7.15 (1H, d, *J* = 7.2, C**H**$_F$Ar), 3.55 (2H, s, C**H**$_{2G}$), 2.91 (2H, t, *J* = 8.0, C**H**$_{2B}$), 2.64 (2H, t, *J* = 8.0, C**H**$_{2A}$), 2.42 (3H, s, C**H**$_3$); ^{13}C NMR (75 MHz, $CDCl_3$) δ 137.2 (**C**H Ar), 136.0 (**C**H Ar), 129.9 (**C**H Ar), 125.8 (**C**H Ar), 124.5 (**C**H Ar), 124.0 (**C**H Ar), 59.8 (**C**H$_x$ alkane), 55.2 (**C**H$_x$ alkane), 46.0 (**C**H$_x$ alkane), 30.0 (**C**H$_x$ alkane).

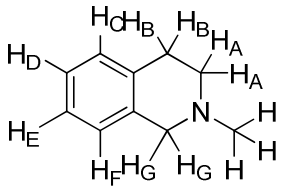

^{1}H NMR assignments

Preparation of 2-methyl-1,2,3,4-tetrahydroisoquinoline – 8 mins

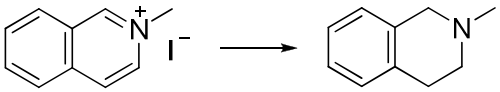

2-Methyl isoquinolinium iodide (3 g, 0.021 mol) in methanol (20 mL) and water (10 mL) was cooled to 0 °C. Sodium borohydride (3 g, 0.072 mol) was added in portions (*c.a* 2 mins) then rapidly heated to reflux for 6 mins. Once cooled the reaction mixture was washed with a saturated aqueous solution of ammonium chloride and extracted into diethyl ether. Concentration *in vacuo* and purification by distillation to afford the title compound as a colourless oil (0.82 g, 27%).

Preparation of 2-chloro-1-(pyridin-3-yl)ethanone[50]

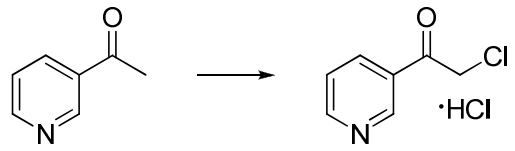

Glacial acetic acid (15 mL) was cooled to 17 ^{o}C with stirring in a sealed test tube and HCl gas bubbled through the solution for two hours. HCl gas was produced by adding conc. sulphuric acid dropwise to sodium chloride with stirring. 3-Acetyl pyridine (1 g, 0.9 mL, 0.0075 mol) was added dropwise to the acetic acid (*c.a* 20 mins) and stirred for one hour. *N*-Chlorosuccinimide (1.0 g, 0.0075 mol) was added to the reaction mixture at 20 ^{o}C with stirring overnight. The reaction mixture was cooled to 15 ^{o}C and the precipitate filtered and then washed with acetic acid (at 17 ^{o}C) then ethyl acetate (at 17 ^{o}C) and dried *in vacuo* to yield the title compound as a white crystalline solid (0.914 g, 71%); m.p 195.5-198 ^{o}C (dec) (lit. 200-201 ^{o}C (dec)); IR v_{max} (DCM)/cm^{-1} 3014 (C-H alkane), 1986 (C-H Ar), 1714 (C=O ketone), 1605 (C=C Ar), 1342 (C-N amine); ^{1}H NMR (300 MHz, DMSO-d_6) δ 9.21 (1H, d, *J* = 3.0, C**H**$_D$ Ar), 8.91 (1H, dd, *J* = 6.0, 3.0, C**H**$_A$Ar), 8.51 (1H, dq, *J* = 6.0, 3.0, 0.6, C**H**$_C$Ar), 7.79 (1H, dd, *J* = 6.0, 3.0, C**H**$_B$Ar), 5.28 (2H, s, C**H**$_{2F}$); ^{13}C NMR (75 MHz, $CDCl_3$) δ 190.5 (**C**O), 149.7 (**C**H Ar), 145.0 (**C**H Ar), 140.1 (**C**H Ar), 131.6 (**C**$_q$H Ar), 126.0 (**C**H Ar), 48.4 (**C**H$_2$).

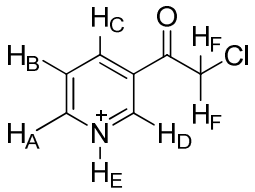

^{1}H NMR assignments

Preparation of 2-chloro-1-(pyridin-3-yl)ethanol[50]

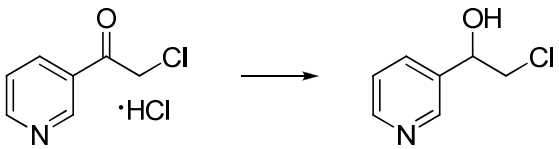

A stirred solution of 2-chloro-1-(pyridin-3-yl)ethanone (0.5 g, 2.6 mmol) in methanol (10 mL) and water (5 mL) was cooled to 0 ^{o}C and sodium borohydride (129 mg, 3.34 mmol) added in portions (*c.a* 30 mins). The solution was allowed to warm to room temperature and stirred for a further two hours. Solvent was removed *in vacuo* and

the residue dissolved in aqueous Na_2CO_3 and extracted with ethyl acetate. The organic layer was dried over sodium sulphate, filtered and dried *in vacuo* to afford a viscous yellow oil. The crude oil was purified by chromatography on silica eluting with hexane/ethyl acetate (5:1) to afford the title compound as viscous colourless oil (0.31 g, 75%); IR v_{max} (DCM)/cm^{-1} 3337 (O-H alcohol), 3014 (C-H alkane), 1986 (C-H Ar), 1605 (C=C Ar), 1342 (C-N amine), 1205 (C-O alcohol); ^{1}H NMR (300 MHz, DMSO-d_6) δ 8.87(1H, dd, *J* = 3.0, 0.6 C**H**$_D$ Ar), 8.01 (1H, dd, *J* = 6.0, 3.0, C**H**$_A$Ar), 7.87 (1H, dq, *J* = 9.0, 3.0, 0.6, C**H**$_C$Ar), 7.30 (1H, dd, *J* = 6.0, 3.0, C**H**$_B$Ar), 4.76 (1H, t, *J* = 7.0, C**H**$_F$), 4.01 (2H, m, C**H**$_E$), 3.55 (1H, m, O**H**); ^{13}C NMR (75 MHz, $CDCl_3$) δ 148.3 (**C**H Ar), 147.6 (**C**H Ar), 138.9 (**C**$_q$H Ar), 134.5 (**C**H Ar), 124.0 (**C**H Ar), 79.2 (**C**O), 49.4 (**C**H_2).

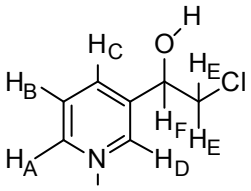

^{1}H NMR assignments

Preparation of 2-amino-1-(pyridin-3-yl)ethanol dihydrochloride[50]

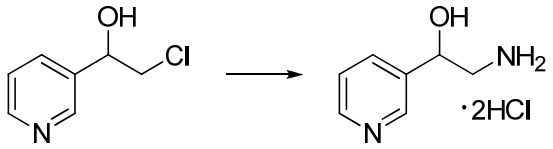

To a solution of 2-chloro-1-(pyridin-3-yl)ethanol (0.2 g, 1.3 mmol) in methanol (10 mL) ammonium hydroxide (30%, 5 mL) was added and stirred at room temperature for 18 hours. Methanol was removed *in vacuo*, one half of the water and ammonia was removed under vacuum distillation. The remaining water and ammonia was removed as an azeotropic vacuum distillate with *n*-butanol. HCl (37%) was added to the solution and concentrated *in vacuo*. The precipitate was re-crystallised from absolute ethanol to yield the title compound as a white crystalline solid (0.09 g, 41%); m.p 197.1-198.3 ^{o}C (lit. 199-201 ^{o}C); IR v_{max} (DCM)/cm^{-1} 3337 (O-H alcohol), 3014 (C-H alkane), 1986 (C-H Ar), 1605 (C=C Ar), 1367 (C-N amine), 1205 (C-O alcohol); ^{1}H NMR (300 MHz, DMSO-d_6) δ 8.86 (1H, dd, *J* = 3.0, 0.6 C**H**$_D$ Ar), 8.09 (1H, dd, *J* = 6.0, 3, C**H**$_A$Ar), 7.77 (1H, m, C**H**$_C$Ar), 7.32 (1H, dd, *J* = 6.0, 3.0, C**H**$_B$Ar),

5.16 (2H, s, N**H**$_2$), 4.76 (1H, t, *J* = 7.0, C**H**$_F$), 3.55 (1H, m, O**H**), 3.30 (2H, m, C**H**$_E$); ^{13}C NMR (75 MHz, $CDCl_3$) δ 148.4 (**C**H Ar), 147.2 (**C**H Ar), 138.1 (**C**$_q$H Ar), 134.8 (**C**H Ar), 124.0 (**C**H Ar), 75.6 (**C**O), 44.0 (**C**H$_2$).

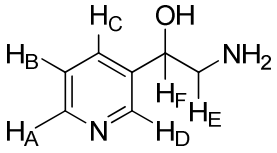

^{1}H NMR assignments

Preparation of nicotinoyl chloride[56]

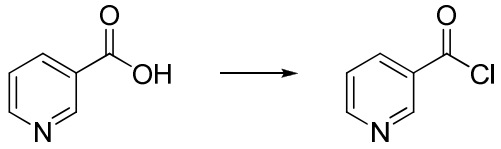

Thionyl chloride (24.6 g, 15 mL, 0.2 mol) was added to nicotinic acid (2 g, 16 mmol) and heated to reflux for 24 hours. The reaction mixture was concentrated *in vacuo*, ether (50 ml) was added and concentrated *in vacuo* twice affording the acid chloride (2.25 g, quant.). The white solid was carried through to the next step without characterisation.

Preparation of N-(1-hydroxy-2-methylpropan-2-yl)nicotinamide[56]

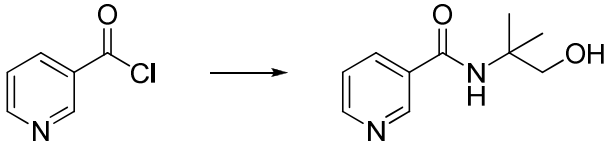

Nicotinoyl chloride (2.25 g, 16 mmol) was dissolved in DCM (20 ml) and added slowly to a cooled solution (0 ^{o}C) of 2-amino-2-methylpropan-1-ol in DCM (20 mL). Once addition was complete the reaction mixture was allowed to warm to room temperature and stirred for 24 hours, concentration *in vacuo* and purification by flash chromatography (silica, AcOEt) afforded the title compound as a white oil (1.3 g, 42%); R_f 0.4 (silica, AcOEt); IR v_{max} (DCM)/cm^{-1} 3310 (N-H), 3270 (O-H), 3021 (C-H, alkene), 2856 (C-H, alkane), 1676 (C=O), 1264 (C-N), 1241 (C-O); ^{1}H NMR (300 MHz, DMSO-d_6) δ 8.88 (1H, s, C**H**$_A$), 8.46 (1H, d, *J* = 7.0,C**H**$_B$), 8.31 (1H, d, *J* = 3.0, C**H**$_D$), 7.56 (1H, dd, *J* = 3.0, 7.0, C**H**$_C$), 6.03 (br, N**H**), 3.62 (1H, s, O**H**), 3.53 (2H, s, C**H**$_E$), 1.30 (6H, s, C**H**$_3$); ^{13}C NMR (75 MHz, DMSO-d_6) δ 164.2 (**C**O), 157.1 (N**C**H),

149.0 (N**C**H), 134.0 (**C**H, Py), 129.5 (**C**H, Py), 126.3 (**C**H, Py), 74.7 (**C**$(CH_3)_2$), 61.0 (**C**OH), 29.9 (**C**H_3).

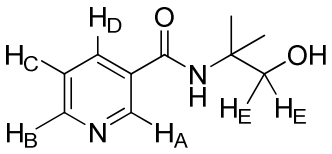

^{1}H NMR assignments

Preparation of 4,4-dimethyl-2-(pyridin-3-yl)-4,5-dihydrooxazole[56]

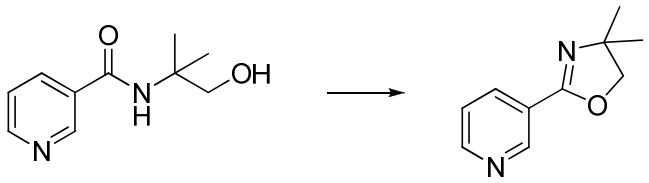

Thionyl chloride (4.9 g, 3 mL, 0.58 mol) was added to N-(1-hydroxy-2-methylpropan-2-yl)nicotinamide (1.3 g, 7 mmol) and stirred at room temperature for 16 hours. The reaction mixture was concentrated *in vacuo*, dissolved in DCM (50 mL) and washed twice with NaOH solution (2 mol, 2 x 30 mL). The organic layer was separated and dried overnight with $MgSO_4$, filtered then concentrated *in vacuo*. Purification by flash chromatography (silica, AcOEt) afforded the title compound as a brown viscous oil (0.32 g, 26%); R_f 0.40 (silica, AcOEt); IR v_{max} (DCM)/cm^{-1} 2968 (CH alkane), 1651 (CN imine), 1591 (C=C Ar), 1386 (CN amine), 1243 (CO ether); ^{1}H NMR (300 MHz, $CDCl_3$) δ 9.02 (1H, s, C**H**$_A$), 8.57 (1H, dd, *J* = 4.9, 1.7 Hz, C**H**$_C$), 8.14 – 8.05 (1H, m, C**H**$_{B/D}$), 7.27 – 7.16 (1H, m, C**H**$_{B/D}$), 4.01 (2H, s, C**H**$_E$), 1.26 (6H, s, C**H**$_3$); ^{13}C NMR (75 MHz, $CDCl_3$) δ 159.2 (**C**N, imine), 150.9 (N**C**H), 148.5 (N**C**H), 134.6 (**C**H, Py), 123.2 (**C**CN), 122.1 (**C**H, Py), 78.1 (**C**H_2), 66.7 (**C**(CH_3)), 27.2 (**C**H_3).

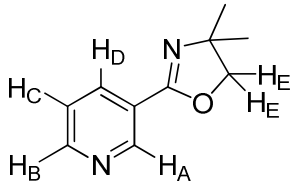

^{1}H NMR assignments

Preparation of 4,4-dimethyl-2-(pyridin-3-yl)-4,5-dihydrooxazole[57]

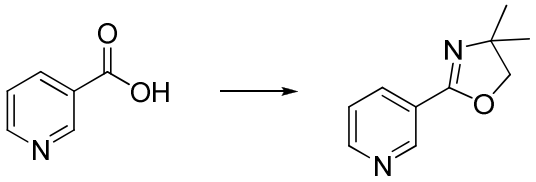

To a stirred solution of nicotinic acid (15 g, 0.12 mol), triphenylphosphine (90 g, 0.34 mol), 2-amino-2,2-dimethylethanol (10.77 g, 11.6 mL, 0.12 mol) and triethylamine (98 g, 135 mL, 0.97 mol) in abs. acetonitrile (100 mL), a solution of carbontetrachloride (37.7 g, 23.8 mL, 0.24 mol) and abs. acetonitrile (36.5 mL) was added at 4 ^{o}C under nitrogen. The solution was warmed to 9 ^{o}C for 4 hours and then allowed to warm to room temperature and stirred for a further 18 hours. The precipitate was filtered and discarded; the dark brown filtrate was concentrated *in vacuo*. The resulting dark brown residue was triturated with hexane (4 x 500 mL portions). The remaining insoluble residue was dissolved in DCM (600 mL), hexane (1000 mL) was added to the solution and the resulting precipitate filtered and washed with hexane (500 mL). The combined filtrates were concentrated *in vacuo* to afford the crude product. Purification by vacuum distillation yielded the title compound as a brown viscous oil (13.96 g, 66%); b.p. 91 ^{o}C (3 mbar).

Preparation of 4,4-dimethyl-2-(4-phenyl-1,4-dihydropyridin-3-yl)-4,5-dihydrooxazole[3]

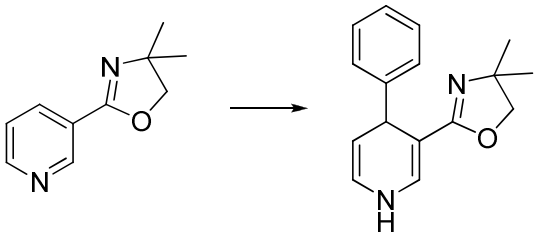

Phenyllithium 1.9 M Cyclohexane/ether (7:3) (46 mL, 0.14 mol, 1.8 equiv) was added to a cooled solution (-78 ^{o}C) of 4,4-dimethyl-2-(pyridin-3-yl)-4,5-dihydrooxazole (13.96 g, 0.08 mol) in anhyd. THF (100 mL) under nitrogen and stirred for 3 hours. The reaction was quenched with water (100 mL) and left to warm to room temperature, ether (300 mL) was added to the reaction mixture. The resulting precipitate was filtered, rinsed with chilled methanol (50 mL) and dried at 40 ^{0}C in a vacuum oven overnight to yield the title compound as a crude white solid (15.7 g,

78%); purification by flash chromatography was attempted with no pure product isolated, the crude solid was taken through to the next step.

Preparation of 4,4-dimethyl-2-(4-phenylpyridin-3-yl)-4,5-dihydrooxazole[3]

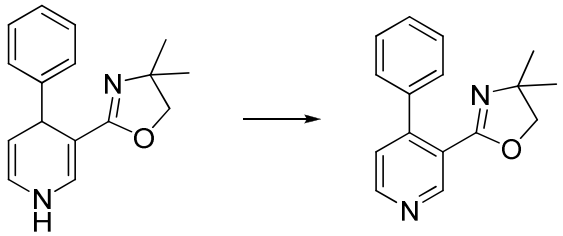

A suspension of 4,4-dimethyl-2-(4-phenyl-1,4-dihydropyridin-3-yl)-4,5-dihydrooxazole (15.7 g, 0.06 mol) and sulphur (16 g, 0.062 mol) in toluene (100 mL) was heated to reflux for 5 hours. The reaction was allowed to cool to room temperature and filtered; the filtrate was concentrated *in vacuo* to yield the crude material. Purification by vacuum distillation afforded the title compound as a viscous oil (12.4 g, 82%); b.p. 153 ^{o}C (3 mbar); IR v_{max} (DCM)/cm^{-1} 2968 (C-H alkane), 1651 (C=N imine), 1636 (C=C Ar), 1243 (C-O ether); ^{1}H NMR (300 MHz, DMSO-d_6) δ 7.98 (1H, s, C**H**$_A$), 7.20 (4H, m, C**H**$_{D/E}$), 7.08 (1 H, m, C**H**$_F$), 6.94 (1H, d, *J* = 8.0, C**H**$_C$), 6.14 (1H, d, 8.0, C**H**$_B$), 4.04 (2H, s, C**H**$_G$), 1.22 (6H, s, C**H**$_3$); ^{13}C NMR (75 MHz, $CDCl_3$) δ 163.1 (**C**N, imine), 152.3 (N**C**H), 150.7 (N**C**H), 148.1 (**C**CH Ar), 138.2 (**C**CH Py), 129.8 (**C**H Ar), 128.1 (**C**H Ar), 127.2 (**C**H Ar), 125.1 (**C**H Py), 78.0 (**C**H$_2$), 71.8 (**C**CH$_3$), 28.0 (**C**H$_3$).

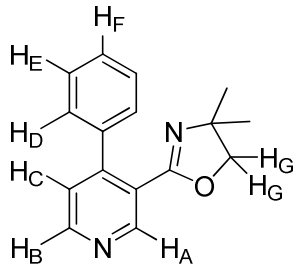

^{1}H NMR assignments

Preparation of 4-phenylnicotinic acid hydrochloride[3]

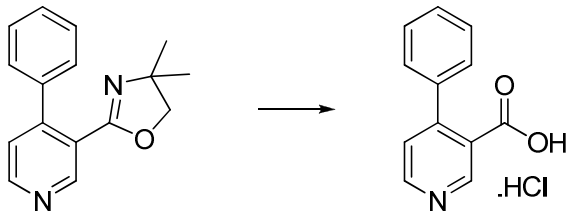

4,4-Dimethyl-2-(4-phenylpyridin-3-yl)-4,5-dihydrooxazole (12.4 g, 0.05 mol) and concentrated HCl (25 mL) were heated to reflux for 24 hours. The mixture was

allowed to cool to room temperature, filtered and the resulting solid washed with chilled 1 mol HCl. The white solid was dried overnight at 40 ^{o}C under vacuum to yield the title compound (10.9 g, 93%); IR ν_{max} (DCM)/cm^{-1} 3333 (O-H), 2963 (C-H alkane), 1672 (C=O), 1636 (C=C Ar), 1243 (C-O ether); ^{1}H NMR (300 MHz, DMSO-d_6) δ 11.05 (1H, s, O**H**), 9.04 (1H, s, C**H**$_A$), 8.87 (1H, d, J = 5.6 Hz, C**H**$_B$), 7.77 (1H, d, J = 5.6 Hz, C**H**$_C$), 7.61 – 7.30 (5H, m, C**H**$_{D,E,F}$); 5.72 (broad signal, N**H**); ^{13}C NMR (75 MHz, DMSO-d_6) δ 164 (**C**O), 157 (**C**CH, Py) 146 (N**C**H), 144 (N**C**H), 138 (**C**CH, Ar), 128 (**C**H, Ar), 127 (**C**H, Ar), 127 (**C**H, Ar), 125 (**C**COOH), 123 (**C**H, Py).

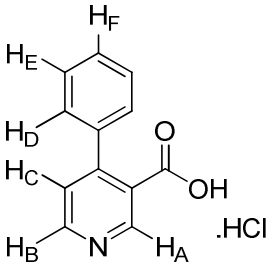

^{1}H NMR assignments

Preparation of 4-phenylnicotinoyl chloride[3]

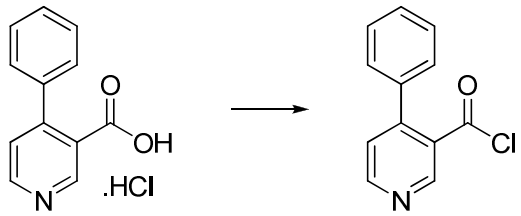

Thionyl chloride (50 mL) was added to 4-phenylnicotinic acid hydrochloride (10.9 g, 46 mmol) and heated to reflux for 24 hours. The mixture was allowed to cool to room temperature and concentrated *in vacuo*, ether (50 mL) was added to the resulting oil and concentrated *in vacuo* two times to yield a viscous colourless oil (10.01 g, quant.). The oil was carried through to the following step without characterisation.

Preparation of cyclohexylmethyl 4-phenylnicotinate[3]

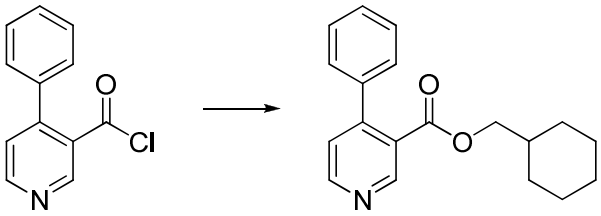

4-Phenylnicotinoyl chloride (10.01 g, 0.046 mol) was diluted in DCM (25 mL) and added slowly to a cooled solution (0 ^{o}C) of cyclohexanemethanol (5.84 g, 6.26 mL, 0.051 mol) and diisopropylethylamine (6.60 g, 8.9 mL, 0.051 mol) in DCM (50 mL). Once addition was complete, the reaction mixture was allowed to warm to room temperature and stirred for 24 hours. The reaction mixture was quenched with aqueous saturated $NaHCO_3$ solution (50 mL) and extracted twice with DCM (2 x 50 mL). The organic layer was dried overnight ($MgSO_4$), filtered and concentrated *in vacuo* to afford the crude product. Purification over silica (eluting with 30% EtOAc:hexane) yielded the title compound as a brown oil (8.01 g, 59%); R_f 0.8 (silica, 30% EtOAc:hexane); IR v_{max} (DCM)/cm^{-1} 3001 (C-H, alkene), 2957 (C-H alkane), 1672 (C=O), 1636 (C=C Ar), 1255 (C-O ether); ^{1}H NMR (300 MHz, $CDCl_3$) δ 9.02 (1H, s, C**H**$_A$), 8.70 (1H, s br, C**H**$_B$), 7.41 (4H, m, C**H**$_{D,E}$), 7.31 (2H, m, C**H**$_{C,F}$), 3.87 (2H, d, *J* = 6.4, C**H**$_G$), 1.72 (1H, m, C**H**$_H$), 1.59 (4H, m, C**H**$_I$), 1.37 (4H, m, C**H**$_J$), 1.20 (2H, m, C**H**$_K$); ^{13}C NMR (75 MHz, $CDCl_3$) δ 166.3 (**C**O), 150.5 (N**C**H), 149.2 (N**C**H), 138.7 (**C**CH, Py), 127.3 (**C**H, Ar), 127.8 (**C**H, Ar), 127.0 (**C**H, Ar), 124.5 (**C**CO), 69.7 (**C**H$_2$), 35.1 (**C**H), 28.3 (**C**H$_2$), 25.2 (**C**H$_2$), 24.0 (**C**H$_2$).

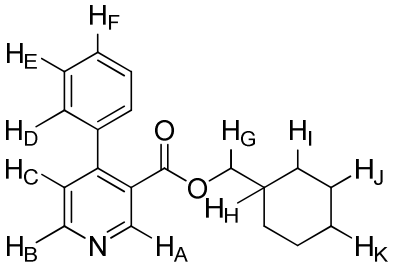

^{1}H NMR assignments

Preparation of 3-((cyclohexylmethoxy)carbonyl)-1-ethyl-4-phenylpyridinium iodide[3]

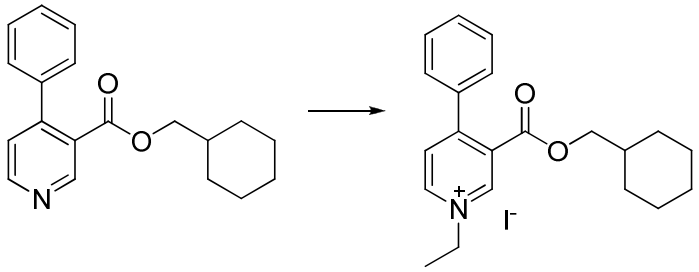

Ethyliodide (9.75 g, 5 mL, 63 mmol) was added to cyclohexylmethyl 4-phenylnicotinate (0.5 g, 1.6 mmol) and heated to reflux for 24 hours. The reaction mixture was then concentrated *in vacuo* to yield the title compound (0.76 g, quant.); IR v_{max} (DCM)/cm^{-1} 2887 (C-H, alkene), 2957 (C-H alkane), 1673 (C=O), 1640 (C=C Ar), 1337 (C-N), 1260 (C-O ether); ^{1}H NMR (300 MHz, $CDCl_3$) δ 9.88 (1H, d, *J* = 6.4, C**H**$_B$), 9.32 (1H, s, C**H**$_A$), 8.12 (1H, d, *J* = 6.4, C**H**$_C$), 7.59 (3H, m, C**H**$_{E,F}$), 7.46 (2H, dd, *J* = 4.0, 2.2, C**H**$_D$), 5.10 (2H, m, C**H**$_L$), 3.95 (2H, d, *J* = 8.4, C**H**$_G$), 1.78 (3H, t, *J* = 7.3, C**H**$_M$), 1.57 (1H, m, C**H**$_H$), 1.36 (4H, m, C**H**$_I$), 1.08 (4H, m, C**H**$_J$), 0.67 (2H, m, C**H**$_K$); ^{13}C NMR (75 MHz, $CDCl_3$) δ 162.3 (**C**O), 157.2 (**C**CH, Py) 145.0 (**C**H, Py), 143.8 (**C**CH, Py), 134.4 (**C**CH, Ar), 130.1 (**C**H, Ar), 129.1 (**C**H, Ar), 129.6 (**C**H, Ar), 128.5 (**C**CO, Py), 127.1 (**C**H, Py), 71.0 (O**C**H$_2$), 56.4 (N**C**H$_2$), 35.6 (**C**H), 28.4 (CH**C**H$_2$), 24.6 (**C**H$_2$), 24.4 (**C**H$_2$), 15.3 (**C**H$_3$).

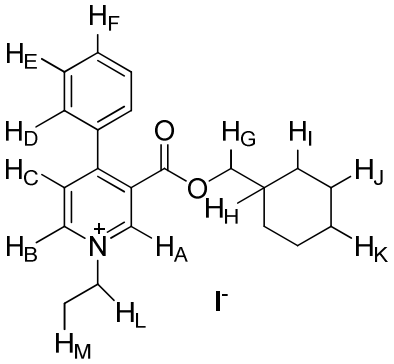

^{1}H NMR assignments

Preparation of cyclohexylmethyl 1-ethyl-4-phenyl-1,2,3,6-tetrahydropyridine-3-carboxylate (2) and cyclohexylmethyl 1-ethyl-4-phenyl-1,2,5,6-tetrahydropyridine-3-carboxylate (3)[3]

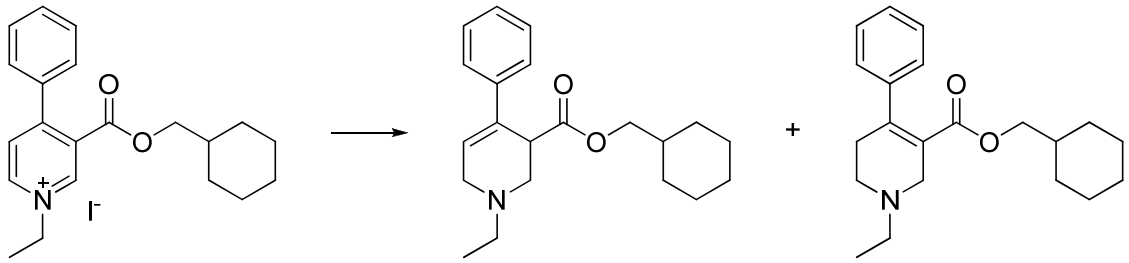

2 **3**

$NaBH_4$ (0.56 g, 15 mmol) was added portion wise to a cooled a solution (0 ^oC) of 3-((cyclohexylmethoxy)carbonyl)-1-ethyl-4-phenylpyridinium iodide (0.75 g, 1.6 mmol) in MeOH (5 mL) and water (5 mL) $NaBH_4$ (0.56 g, 15 mmol) with stirring. The reaction mixture was allowed to warm to room temperature and stirred for 1.5 hours. The reaction was quenched with conc. HCl (4 mL) and neutralised with NH_4OH solution (pH 8). The mixture was extracted 3 times with EtOAc, concentration *in vacuo* afforded a mixture of **2** and **3** as a 1:1 mixture (0.483 g, 92%). Purification by flash chromatography yielded **2** (0.034 g, 6%) and **3** (0.038 g, 7%).

Compound **2**: R_f 0.45 (silica, 25% EtOAc:Hexane); IR v_{max} (DCM)/cm^{-1} 2890 (C-H, alkene), 2950 (C-H alkane), 1675 (C=O), 1652 (C=C, alkene),1641 (C=C Ar), 1320 (C-N), 1266 (C-O ether); ^1H NMR (300 MHz, $CDCl_3$) δ 7.43 (5H, m, C**H**$_{D,E,F}$), 3.83 (1H, s, C**H**$_A$), 3.67 (2H, d, *J* = 11.4, C**H**$_G$), 3.55 (1H, d, *J* = 7.9, C**H**$_B$), 3.43 (2H, m, C**H**$_L$), 3.25 (3H, m, C**H**$_M$), 3.07 (1H, d, *J* = 7.9, C**H**$_C$), 3.88 (2H, m, C**H**$_K$), 1.46 (8H, m, C**H**$_{I,J}$); ^{13}C NMR (75 MHz, $CDCl_3$) δ 167.6 (**C**=O), 144.2 (**C**C, Py), 142.0 (**C**C, Ar), 128.3 (**C**H, Ar), 126.0 (**C**H, Ar), 121.0 (**C**CO), 63.6 (O-**C**H_2), 52.5 (**C**H, Py), 51.9 (**C**H_2, Et), 48.0 (**C**H, Py), 36.3 (**C**H, Hex), 28.2 (**C**H, Py), 24.6 (**C**H_2, Hex), 17.1 (**C**H_2, Hex), 14.2 (**C**H_2, Hex), 13.1 (**C**H_3); mass: *m/z* (%) = 327.23 (100).

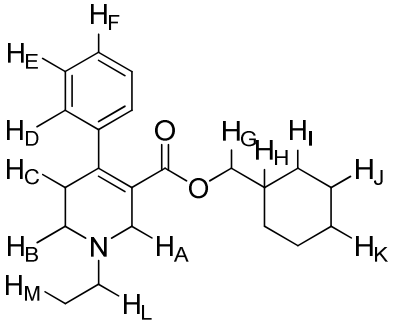

^1H NMR assignments

Compound **3**: R_f 0.3 (silica, 25% EtOAc:Hexane); IR v_{max} (DCM)/cm^{-1} 2866 (C-H, alkene), 2953 (C-H alkane), 1672 (C=O), 1655 (C=C, alkene),1645 (C=C Ar), 1313 (C-N), 1256 (C-O ether); ^{1}H NMR (300 MHz, $CDCl_3$) δ 7.27 (5H, m, C**H**$_{D,E,F}$), 6.09 (1H, t, *J* = 3.0, C**H**$_C$), 4.05 (2H, m, C**H**$_G$), 2.92 (3H, m, C**H**$_{A,N}$), 2.80 (2H, m, C**H**$_B$), 2.39 (2H, q, *J* = 12, C**H**$_L$), 2.06 (1H, m, C**H**$_H$), 1.58 (4H, m, C**H**$_I$), 1.52 (4H, m, C**H**$_J$), 1.37 (2H, m, C**H**$_K$), 1.15 (3H, m, C**H**$_M$); ^{13}C NMR (75 MHz, $CDCl_3$) δ 167.2 (**C**=O), 144.7 (**C**C, Py), 142.2 (**C**C, Ar), 128.0 (**C**H, Ar), 126.3 (**C**H, Ar), 115.1 (**C**=C, Py), 63.8 (O-**C**H_2), 52.6 (**C**H, Py), 51.5 (**C**H_2, Et), 48.0 (**C**H, Py), 36.3 (**C**H, Hex), 28.1 (**C**H, Py), 24.2 (**C**H_2, Hex), 17.5 (**C**H_2, Hex), 14.3 (**C**H_2, Hex), 13.9 (**C**H_3); mass: *m/z* (%) = 327.22 (100).

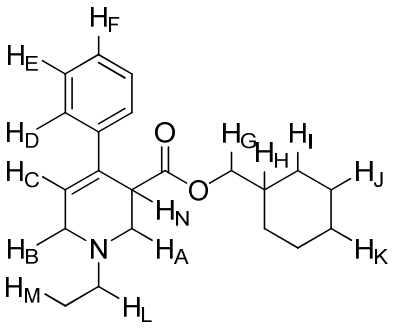

^{1}H NMR assignments

All physical and spectroscopic data were consistent with those reported.

6.1 MOLECULAR MODELLING

Sybyl version X (Tripos - Sybyl X) was used for all construction of analogues and their resulting conformers, COMFA (comparative molecular field analysis) and PLS (partial least square) analyses. Prior to minimisations, all analogues were generated from similar molecules of known X-ray crystallographic structures obtained from the Conquest (linux OS) database.

Protein homology modelling was performed initially in clusta w (web based sequence alignment tool) and verified against multalin (web based sequence alignment tool) to determine a primary sequence with adequate similarity, with primary structures sourced from the protein data bank. Determination of secondary and tertiary structures was obtained utilising atome (web based modelling tool) before importing into Sybyl X to carry out docking studies.

GENERATION OF ANALOGUES

Two suitable structures were sourced from Conquest database as a suitable starting point to construct a range of analogues for the docking studies (Figure 6.0).

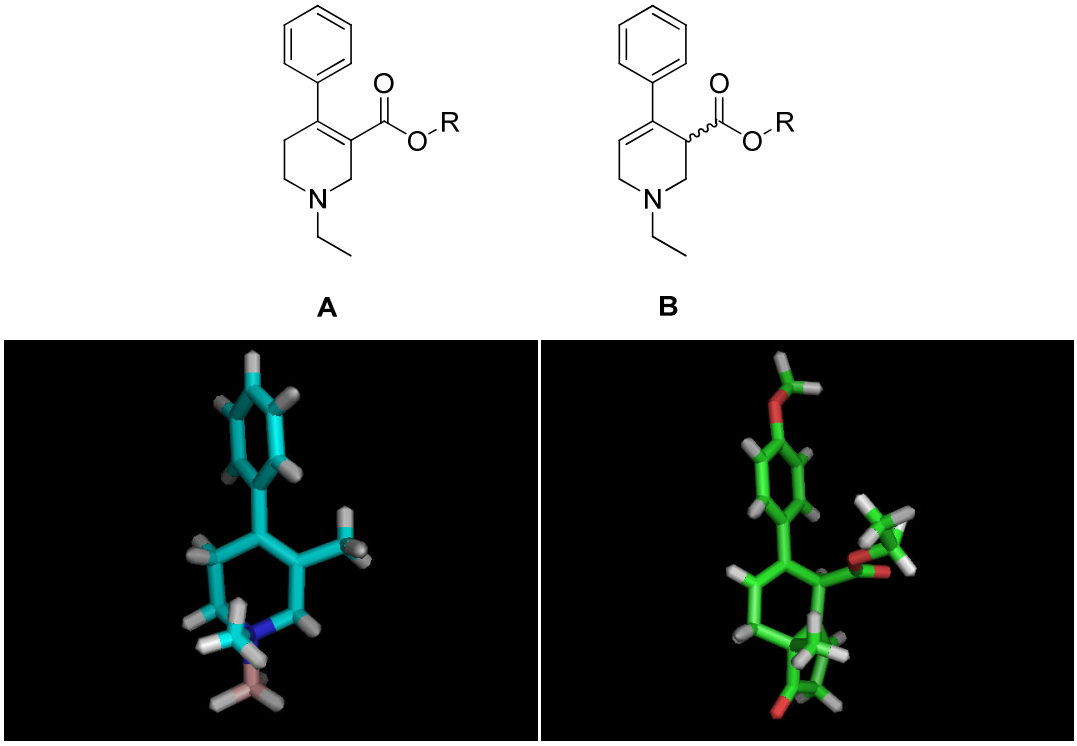

Figure 6.0 X-ray structures for modelling of analogues A (left) and B (right) respectively.

A range of analogues were selected from the original publication by Augelli-Szafran *et al* (Table 6.01).

Compound	Motif	Isomer	R	IC_{50} (nM)
4	B	R	$(CH_2)_5CH_3$	27.3
5	B	S	$(CH_2)_5CH_3$	27.3
6	A	-	$CH_2C_6H_{11}$	14.5
7	A	-	C_6H_{11}	18.1
8	B	R	C_6H_{11}	16.9
9	B	S	C_6H_{11}	16.9
10	A	-	$(CH_2)_2Ph$	9.6
11	A	-	$CH_2CH(CH_3)_2$	120.5

12	B	R	$CH_2CH(CH_3)_2$	128
13	B	S	$CH_2CH(CH_3)_2$	128
14	A	-	$(CH_2)_9CH_3$	106.1
15	B	R	$(CH_2)_2$Ph-*p*-OCH_3	159
16	B	S	$(CH_2)_2$Ph-*p*-OCH_3	159
17	A	-	CH_3	2308
18	B	R	CH_3	33117
19	B	S	CH_3	33117
20	A	-	Ph	1819
21	A	-	CH_2CH_3	888
22	A	-	$(CH_2)_2$Ph-*p*-OCH_3	1941

Table 6.01 Analogues selected for modelling analysis

ENERGY MINIMISATION

All minimisations were carried out using a Fletcher-Powell method, considering both electrostatic and Van der Waals forces. The end point of the process was determined by the gradient with a force field parameter of 0.05 kcalmol^{-1}, typically the end point was reached within 500 iterations. The bond rotations considered and their respective degrees of freedom are defined in Figure 6.01 and Table 6.01.

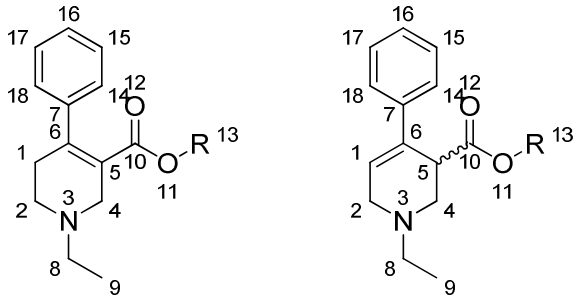

Figure 6.01 Analogues A and B (atom labelled).

	Bond	Degree of Freedom		Bond	Degree of Freedom
A	1-2	10^o	B	1-2	10^o
A	2-3	bond cleavage*	B	2-3	10^o

A	3-4	10^o	B	3-4	bond cleavage*
A	4-5	10^o	B	4-5	10^o
A	1-6	10^o	B	5-6	10^o
A	6-7	60^o	B	6-7	60^o
A	3-8	30^o	B	3-8	30^o
A	8-9	30^o	B	8-9	30^o
A	5-10	60^o	B	5-10	60^o
A	10-11	180^0	B	10-11	180^0
A	11-13	30^o	B	11-13	30^o

*A single cleavable bond is defined in the pyridinal ring to allow the software to ring flip to find the lowest energy state.

Table 6.01 Defined degrees of freedom for conformational analysis.

The conformational analysis afforded a range of structures for each analogue, the relative conformational energy was calculated for all conformers and the lowest energy conformation was selected to proceed into the docking experiment. A full database of the data obtained from the conformational analysis can be found in Appendix 1.

COMFA analysis was performed on all analogues by identification of pharmacophore (Figure 6.02) and superimposing the analogues on each other (Appendix 1). A summary of the results are given in Table 6.02.

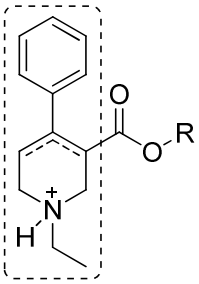

Figure 6.02 Identified pharmacophore for COMFA analysis

Compound	Motif	Isomer	COMFA Score	IC_{50} (nM)
4	B	R	81	27.3
5	B	S	82	27.3
6	A	-	80	14.5

7	A	-	78	18.1
8	B	R	77	16.9
9	B	S	75	16.9
10	A	-	82	9.6
11	A	-	73	120.5
12	B	R	67	128
13	B	S	68	128
14	A	-	94	106.1
15	B	R	86	159
16	B	S	83	159
17	A	-	61	2308
18	B	R	62	33117
19	B	S	60	33117
20	A	-	71	1819
21	A	-	65	888
22	A	-	83	1941

Table 6.02 Summary of results from COMFA analysis

PROTEIN HOMOLOGY MODELLING

Primary sequences of β2 adrenergic and M1 muscarinic receptors were obtained from protein data bank (PDB) and initial sequence homology performed by blast p (web based homology program) yielding a 95% agreement in the primary sequence. The sequence alignment was performed by two independent programs (mustalin and clusta w) and gave good agreement with helical alignment and conservation of di-sulfide bridges.

The aligned sequences from the analysis by clusta w was taken forward to construct a model of the M1 muscarinic receptor based on β2 adrenergic receptor. The aligned sequence (Appendix 2) was submitted to atome (web based program) to construct an initial model for M1 muscarinic receptor. Upon detailed analysis of helical structures it was deemed a suitable model with no need to insert point mutations. There was good conservation of all 7 helices and di-sulfide bridges

(Figure 6.03) (Appendix 2). Figure 6.03 is orientated with the top of the model extracellular and the bottom intracellular, note the incorporation additional protein structure intracellular between helix 6 and 7, this was required to obtain the initial X-ray structure of β2 adrenergic receptor and thus was conserved in M1 muscarinic model. This in no way impedes the binding of compounds as the active site is located extracellular helix 3.

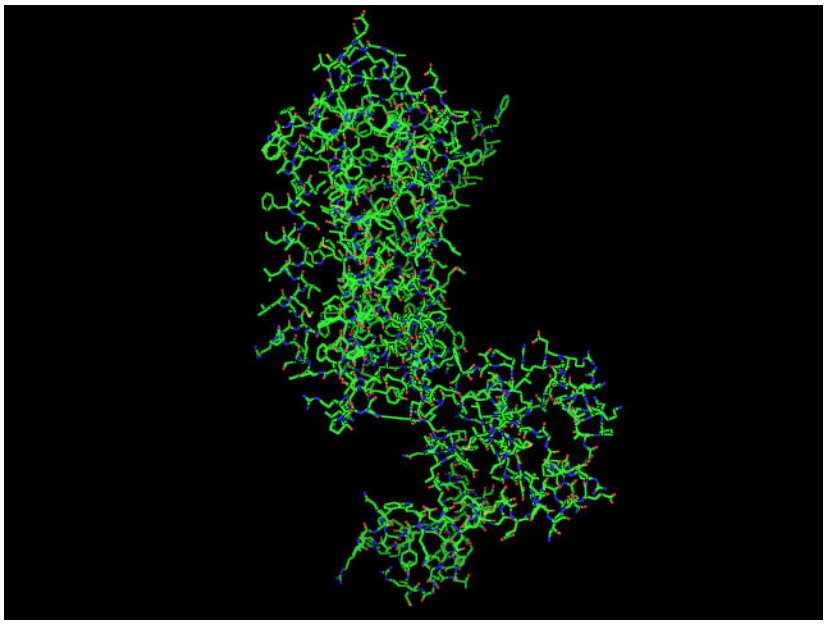

Figure 6.03 Model of M1 muscarinic receptor

DOCKING STUDIES

Key residues identified to generate the protomol (area in which molecule is to be docked) were defined: aspartic acid (105) and tyrosine (381). Residues within 10 angstrom radius of aspartic acid (105) were defined as important, yielding the protomol (Appendix 2).

Each analogue (in its protonated form – Figure 6.02) was docked into the active site and evaluated with respect to electrostatic and Van der Waals interactions within the protomol. A summary of the scores generated are given in Table 6.03.

Compound	Motif	Isomer	Docking Score	IC_{50} (nM)
4	B	R	5.04	27.3
5	B	S	4.34	27.3
6	A	-	6.84	14.5
7	A	-	4.46	18.1

8	B	R	-*	16.9
9	B	S	-*	16.9
10	A	-	5.12	9.6
11	A	-	4.53	120.5
12	B	R	4.23	128
13	B	S	3.61	128
14	A	-	5.45	106.1
15	B	R	3.81	159
16	B	S	5.64	159
17	A	-	2.48	2308
18	B	R	3.53	33117
19	B	S	2.65	33117
20	A	-	3.94	1819
21	A	-	3.93	888
22	A	-	4.88	1941

*Compounds **8** and **9** were rejected from the docking study due to a steric clash with neighbouring residues.

Table 6.03 Summary results of docking studies

All data from docking studies can be found in Appendix 2.

ABBREVIATIONS

Abs.	Absolute	
Ac	Acetyl	
AD	Alzheimer's disease	
Ar	Aromatic	
BBB	Blood brain barrier	
Boc	*Tert*-butylcarbonate	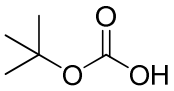
b.p.	Boiling point	
CCR	Chemokine receptor	
CNS	Central nervous system	
conc.	Concentrated	
C_q	Quaternary carbon	
DCM	Dichloromethane	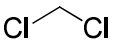
DMA	Dimethylacetamide	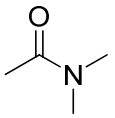
DMF	Dimethylformamide	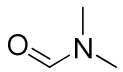
Et	Ethyl	
FDG	2-fluoro-2-deoxyglucose	
IC_{50}	Half maximal inhibitory concentration	
K_i	Dissociation constant	
LAH	Lithium aluminium hydride	
mAChRs	Muscarinic acetylcholine receptor	
Me	Methyl	
m.p.	Melting point	
NBS	*N*-bromosuccinimide	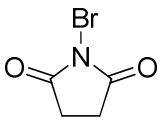
NCS	*N*-chlorosuccinimide	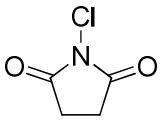

NMR	Nuclear magnetic resonance
PET	Positron emission tomography
Py	Pyridine 
Quat.	Quaternary
RSA	Retro-synthetic analysis
SAR	Structure-activity relationship
TEA	Triethyl amine 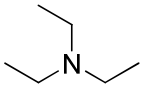
Tf	Trifluoromethane sulfonate 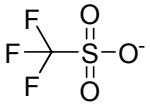
THF	Tetrahydrofuran 
TLC	Thin layer chromatography

REFERENCES

[1] Serdons, K.; Verbruggen, A.; Bormans, G. M. *Methods.* **2009**, *48*, 104-111.

[2] Malviya, M.; Kumar, Y. C. S.; Mythri, R. B.; Venkateshappa, C.; Subhash, M. N.; Rangappa, K. S. *Bioorg. Med.Chem.* **2009**, *17*, 5526-5534.

[3] Augelli-Szafran, C; *et al*. *J. Med. Chem.* **1999**, 42, 356-363.

[4] Saha, G. *Basics of PET Imaging*; 1st Edition., Springer; 2005.

[5] URL: http://images.suite101.com/263636_petimage.jpg

[6] Fowler, J. S.; Ido, T. *Semin. Nucl.Med.* **2002**, *32*, 6-12.

[7] Koziorowski, J. *Appl. Radia. Isot*. **2010**, *68*, 1740-1742.

[8] Reivich, M.; Kuhl, D.; Wolf, A.; Greenberg, J.; Phelps, M.; Ido, T.; Casella, V.; Fowler, J.; Gallagher, B.; Hoffman, E.; Alavi, A.; Sokoloff, L. *Acta Neurologica Scandinavica.* **1977**, *56*, 190-191.

[9] Sullivan, B. P.; Meyer, T. J. *Organometallics.* **1986**, *5*, 1500-1502.

[10] Welch, M. J.; Kilbourn, M. R. *J. Lab. Compd. Radiopharm.* **1985**, *22*, 1193-1200.

[11] Saha, G. B. *Basics of PET Imaging*; Springer, 2005.

[12] Kabalka, G. W.; Lambrecht, R.; Sajjad, M.; Fowler, J.; Kunda, S.; McCollum, G.; MacGregor, R. *Int. J. Appl. Radia. Isot.* **1985**, *36*, 853-855.

[13] Wieland, B.; *et al*. *Appl. Radia. Isot.* **1991**, *42*, 1095-1098.

[14] Hagooly A.; Rossin, R.; Welch, M. *Handb. Exp. Pharmacol.* **2008**, *185*, 93-129.

[15] Schnur, D. M. *Current Opinion in Drug Discovery & Development.* **2008**, *11*, 375-380.

[16] Marechal, E. *Combinatorial Chemistry & High Throughput Screening* **2008**, *11*, 583-586.

[17] Brookmeyer, R.; Gray, S.; Kawas, C. *Am. J. Public Health* **1998**, *88*, 1337-1342.

[18] Yokel, R. A. *Neurotoxicology.* **2000**, *21*, 813-828.

[19] Gokhan-Kelekci, N.; *et al. Bioorg. Med.Chem.* **2007**, *15*, 5775-5786.

[20] Society, Alzheimers. s. 2007. *(Accessed August 2010)* URL: http://www.alzheimers.org.uk/site/scripts/documents_info.php?documentID=100

[21] Schneider, J.; Murray, J.; Banerjee, S.; Mann, A. *Int. J. Geriatric Psychiatry* **1999**, *14*, 651-661.

[22] Palmer, A. M. *Trends Pharmacol. Sci.* **2002**, *23*, 426-433.

[23] Meek, P. D.; McKeithan, E. K.; Schumock, G. T. *Pharmacotherapy.* **1998**, *18*, 68-73.

[24] Tiraboschi, P.; Hansen, L. A.; Thal, L. J.; Corey-Bloom, J. *Neurology.* **2004**, *62*, 1984-1989.

[25] Health, N. I. o.; Aging, N. I. o.; Alzheimer's Disease Education and Referral (ADEAR) Center: 2006. (*Accessed August 2010)* URL: http://www.nia.nih.gov/NR/rdonlyres/63B5A29C-F943-4DB7-91B4-0296772973F3/0/CanADbePrevented.pdf

[26] Rang, H.; Dale, M.; Ritter, J. *Pharmacology*; 5th Edition ed.; Elsevier Churchill Livingstone, 2003.

[27] Uchimura, N.; North, R. A. *J. Physiology –London.* **1990**, *422*, 369-380.

[28] Eglen, R. M.; Choppin, A.; Watson, N. *Trends Pharmacol. Sci.* **2001**, *22*, 409-414.

[29] Bradley, K. N. *Pharmacology & Therapeutics.* **2000**, *85*, 87-109.

[30] Abrams, P.; Freeman, R.; Anderstrom, C.; Mattiasson, A. *Br. J. Urol.* **1998**, *81*, 801-810.

[31] Carmine, A. A.; Brogden, R. N. *Drugs.* **1985**, *30*, 85-126.

[32] Levey, A. I.; Kitt, C. A.; Simonds, W. F.; Price, D. L.; Brann, M. R. *J. Neurosci.* **1991**, *11*, 3218-3226.

[33] Ladner, C. J.; Lee, J. M. *Exp. Neurol.* **1999**, *158*, 451-458.

[34] Tsang, S.; Lai, M.; Kirvell, S.; Francis, P.; Esiri, M.; Hope, T.; Chen, C.; Wong, T. *Neurobiology of Aging.* **2006**, *27*, 1216-1223.

[35] Felder, C. C.; Bymaster, F. P.; Ward, J.; DeLapp, N. *J. Med. Chem.* **2000**, *43*, 4333-4353.

[36] Ghelardini, C.; Galeotti, N.; Lelli, C.; Bartolini, A. *Farmaco.* **2001**, *56*, 383-385.

[37] Saikia, J. R.; Schneeweiss, F. H. A.; Sharan, R. N. *Cancer Lett.* **1999**, *139*, 59-65.

[38] Panouse, J. J. *Comptes Rendus Hebdomadaires Des Seances De L Academie Des Sciences.* **1951**, *233*, 1200-1202.

[39] Kinoshita, N.; Kawasaki, T.; Hamana, M. *Chem. Pharma. Bull.* **1962**, *10*, 753.

[40] Kozello, I. A.; Gasheva, A. Y.; Khmelevsky, V. I. *Khimiko-Farmatsevticheskii Zhurnal.* **1976**, *10*, 90-91.

[41] Sauerberg, P.; Kindtler, J. W.; Nielsen, L.; Sheardown, M. J.; Honore, T. *J. Med. Chem.* **1991**, *34*, 687-692.

[42] Ward, J. S.; Merritt, L.; Klimkowski, M.; Lamb, L.; Mitch, C.; Bymaster, F.; Sawyer, B.; Shannon, H.; Olesen, P. *J. Med. Chem.* **1992**, *35*, 4011-4019.

[43] Wijtmans, R.; Vink, M. K. S.; Schoemaker, H. E.; van Delft, F. L.; Blaauw, R. H.; Rutjes, F. *Synthesis-Stuttgart.* **2004**, 641-662.

[44] Kumar, Y. C. S.; Sadashiva, M. P.; Rangappa, K. S. *Tetrahedron Lett.* **2007**, *48*, 4565-4568.

[45] Kumar, Y.; Malviya, M.; Chandra, J.; Sadashiva, C.; Kumar, C.; Prasad, S.; Prasanna, D.; Subhash, M.; Rangappa, K. *Bioorg. Med. Chem.* **2008**, *16*, 5157-5163.

[46] Malviya, M.; Kumar, Y. C. S.; Asha, D.; Chandra, J.; Subhash, M. N.; Rangappa, K. S. *Bioorg. Med. Chem.* **2008**, *16*, 7095-7101.

[47] Sadashiva, C. T.; Chandra, J.; Kavitha, C. V.; Thimmegowda, A.; Subhash, M. N.; Rangappa, K. S. *Eur. J. Med. Chem.* **2009**, *44*, 4848-4854.

[48] Liebner, F.; Schmid, P.; Adelwohrer, C.; Rosenau, T. *Tetrahedron.* **2007**, *63*, 11817-11821.

[49] Zindell, R.; Riether, D.; Bosanac, T.; Berry, A.; Gemkow, M.; Ebneth, A.; Lobbe, S.; Raymond, E.; Thome, D.; Shih, D.; Thomson, D. *Bioorg. Med. Chem. Lett.* **2009**, *19*, 1604-1609.

[50] Perrone, M. G.; Santandrea, E.; Giorgio, E.; Bleve, L.; Scilimati, A.; Tortorella, P. *Bioorg. Med. Chem.* **2006**, *14*, 1207-1214.

[51] Duquette, J.; Zhang, M. B.; Zhu, L.; Reeves, R. S. *Organic Process Research & Development.* **2003**, *7*, 285-288.

[52] Vorbrüggen, H; Krolikiewicz, K. *Tetrahedron*. **1993**, 49, 9353-9372.

[53] Gourand, F.; Mercey, G.; Ibazizene, M.; Tirel, O.; Henry, J.; Levacher, V.; Perrio, C.; Barre, L. *J. Med. Chem.* **2010**, 53, 1281-1287

[54] Kosower, E. *J. Am. Chem. Soc.* **1955**, 77, 3883-3885

[55] Li, C., Harpp, D. *Tetrahedron Lett.* **1990**, 31, 6291-6294

[56] Robert, N.; Bonneau, A.; Hoarau, C.; Marsais, F. *Org. Lett.* **2006**, 8, 6071-6074

[57] Rosi, S.; Pert, C. B.; Ruff, M. R.; McGann-Gramling, K.; Wenk, G. L. *Neuroscience.* **2005**, *134*, 671-676.

APPENDIX 1

- Database of comformers constructed with calculated physical data.

APPENDIX 2

- Protein homology modelling – sequence alignment, model files, results of docking study.